An outflow in the Seyfert ESO 362-G18 revealed by Gemini-GMOS/IFU Observations

Pedro Humire R.

Universidad de Concepción

September 6, 2017

Outline

1. This research
   - Observation
   - Goals
2. Results
   - Data processing and analysis
   - Single Gaussian fitting results
   - Double Gaussian Fitting results
   - Feeding vs. feedback
3. Comparison with other works
   - Comparison with other works: Kinetic power, kinematic disturbances and dusty structures
4. Summary

DEPARTAMENTO de ASTRONOMÍA UNIVERSIDAD DE CONCEPCIÓN

AGNs black hole accretion rate:

$$0.1 - 100 M_{\odot} yr^{-1} \quad (1)$$

Salpeter time:

$$t_s = \frac{\sigma_T c}{4\pi G m_P} \approx 4.5 \times 10^7 yr \quad (2)$$

From equations (1) and (2), it's required

$$\approx 10^6 - 10^{10} M_{\odot} \quad !!$$

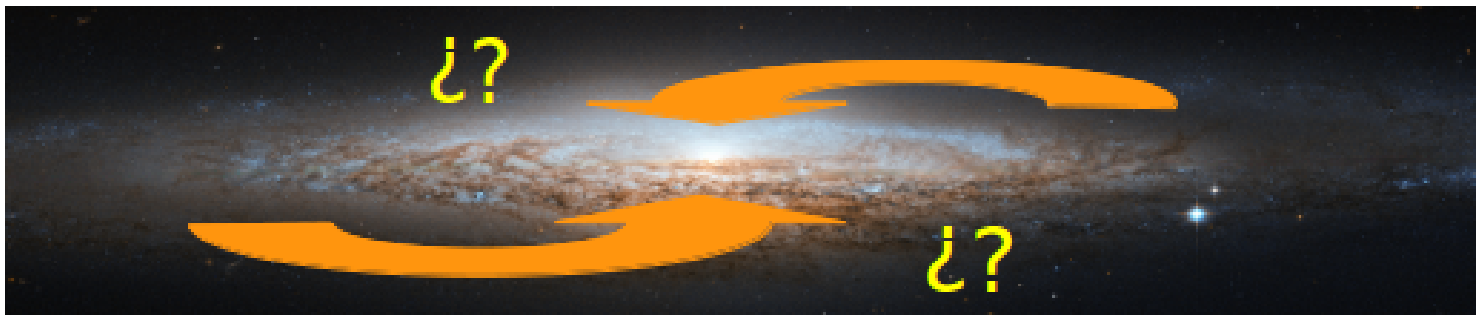

DEPARTAMENTO de ASTRONOMÍA UNIVERSIDAD DE CONCEPCIÓN

Dynamical mechanisms for fueling AGN:

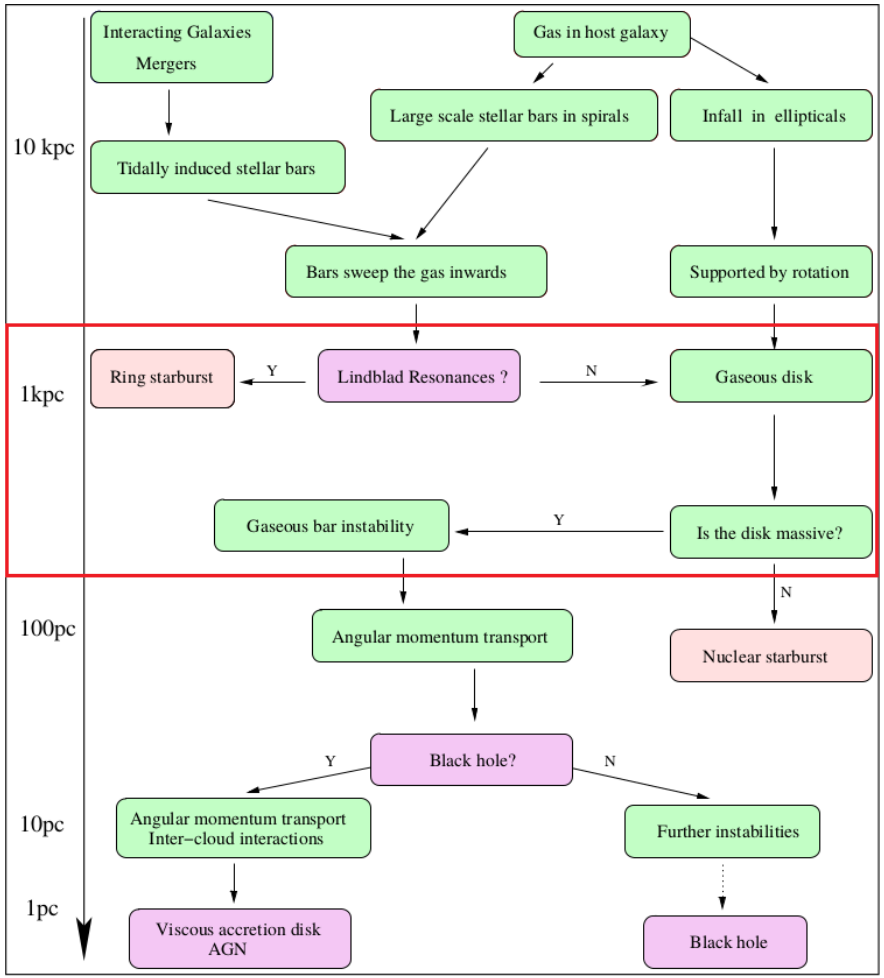

(Fathi, 2004, and references therein)

DEPARTAMENTO de ASTRONOMÍA UNIVERSIDAD DE CONCEPCIÓN

Observation

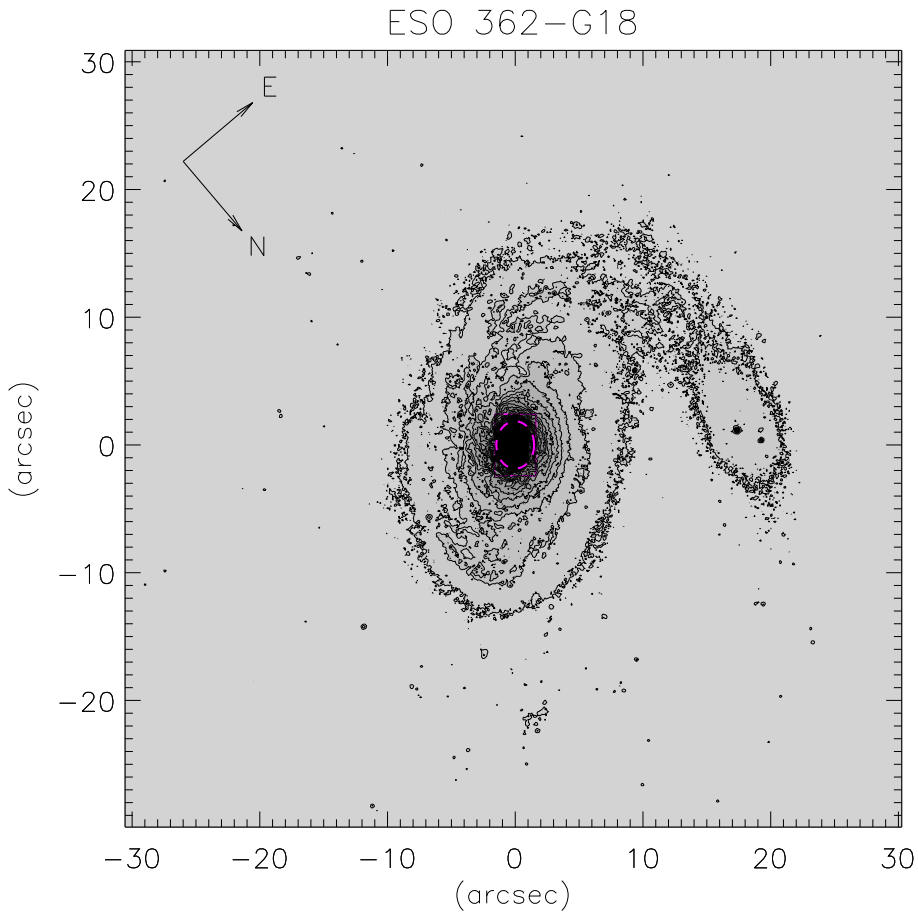

Object name (ESO/MCG)
362-G18/05-13-017
EquJ2000.0 (RA/DEC)
05h19m35.8s/-32d39m27s
Velocity/Redshift (km/s z)
3731/0.012445
$D_L = 52.1$ Mpc
$D_\theta = 50.8$ Mpc
$D_{com} = 51.5$ Mpc

Structure map of ESO 362-G18. The ellipse denotes a circumnuclear ring inclined with the adopted inclination of the galaxy.

DEPARTAMENTO de ASTRONOMÍA UNIVERSIDAD DE CONCEPCIÓN

Immediate Goals

- ESO 362-G18 at 75 km s^{-1} and 160 pc resolution
- Stellar vs. gaseous kinematics
- Kinematics: rotation + inflow + outflow
- Dusty structures
- Complement this study to a larger sample of the group ($\sim$40 galaxies + literature)...

Larger Goals

- Give better constrains for future hydrodynamic simulations.
- Find out what is the typical fraction of the total energy in AGNs that comes from accretion onto the SMBH.
- Confirm or rule out differences between active and non-active galaxies proposed so far.
- Know what are the preferred structures for transporting material to the nucleus in galaxies with active nuclei

DEPARTAMENTO de ASTRONOMÍA UNIVERSIDAD DE CONCEPCIÓN

Different Spectra of ESO 362-G18

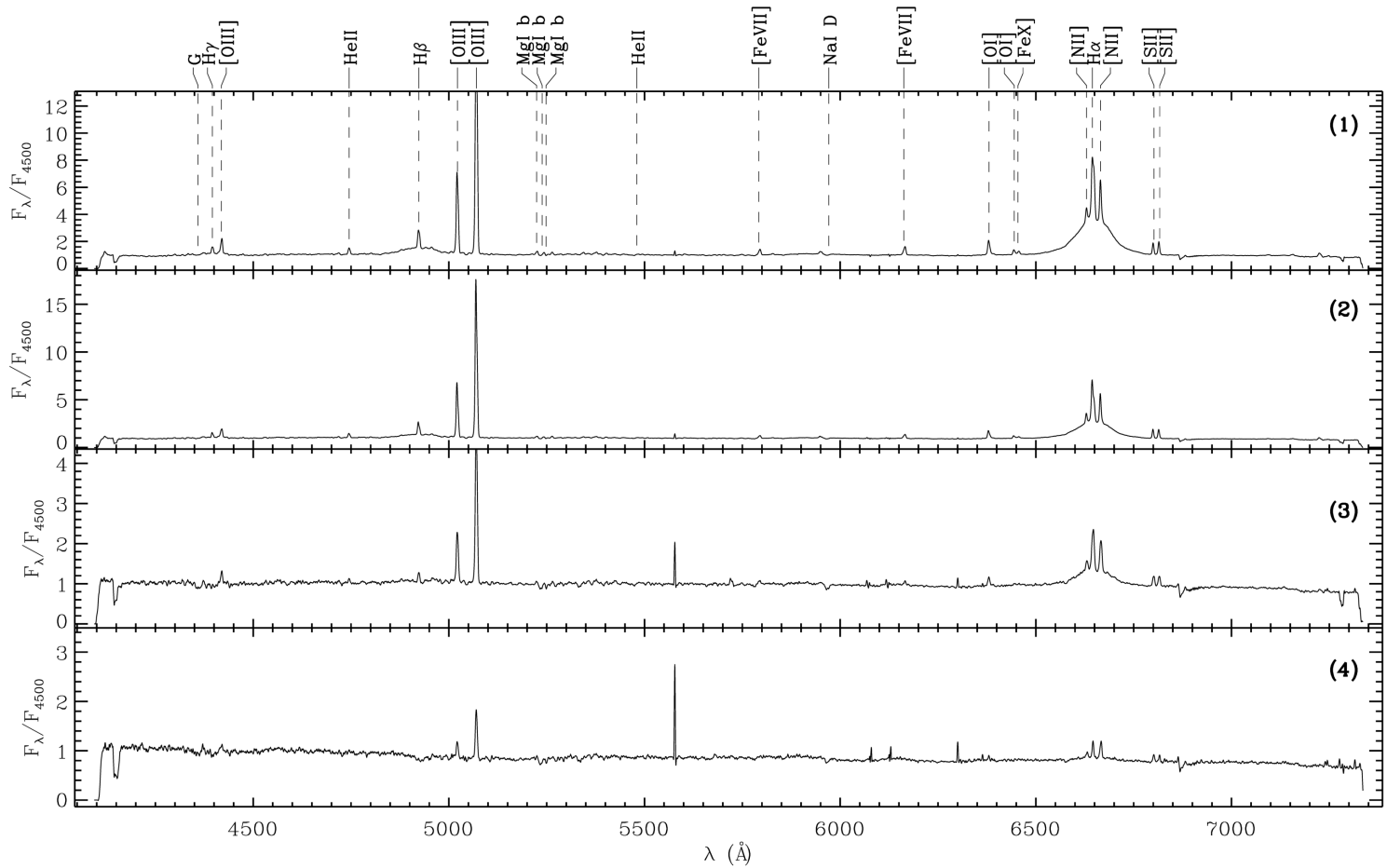

Some ESO 362-G18 spectra.

Stellar Kinematics

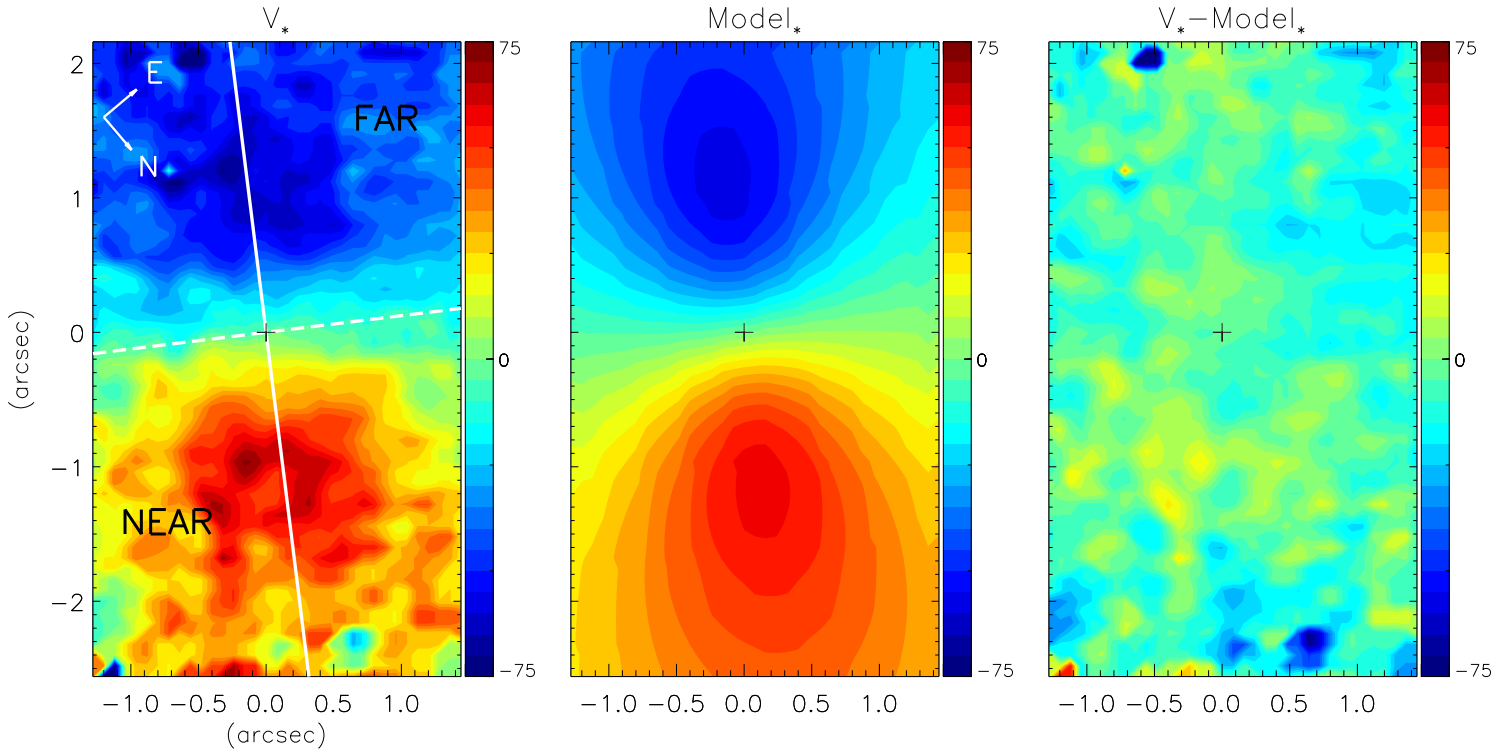

Observed stellar velocity field (km s^{-1}), stellar rotation model (Bertola et al., 1991) and residual.

Gaseous kinematics

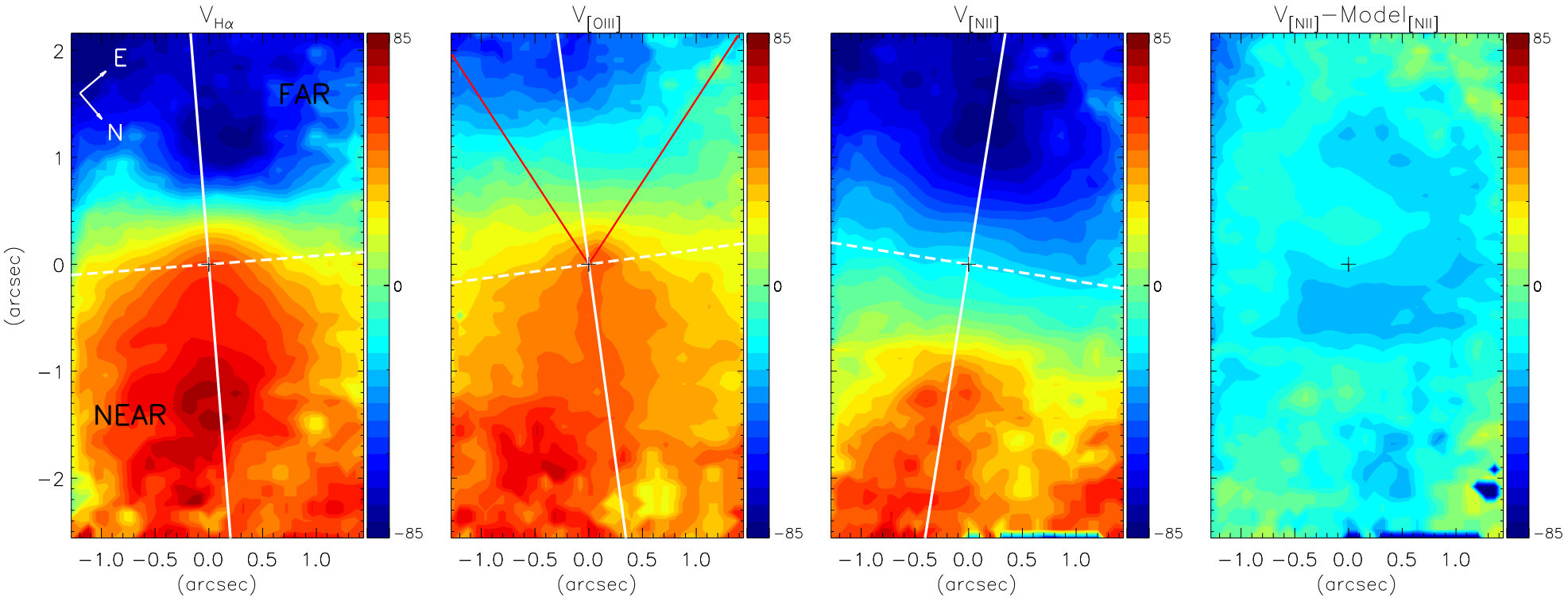

Hα, [O III] and [N II] velocity fields (km s^{-1}) and [N II] residual

Radial Velocities

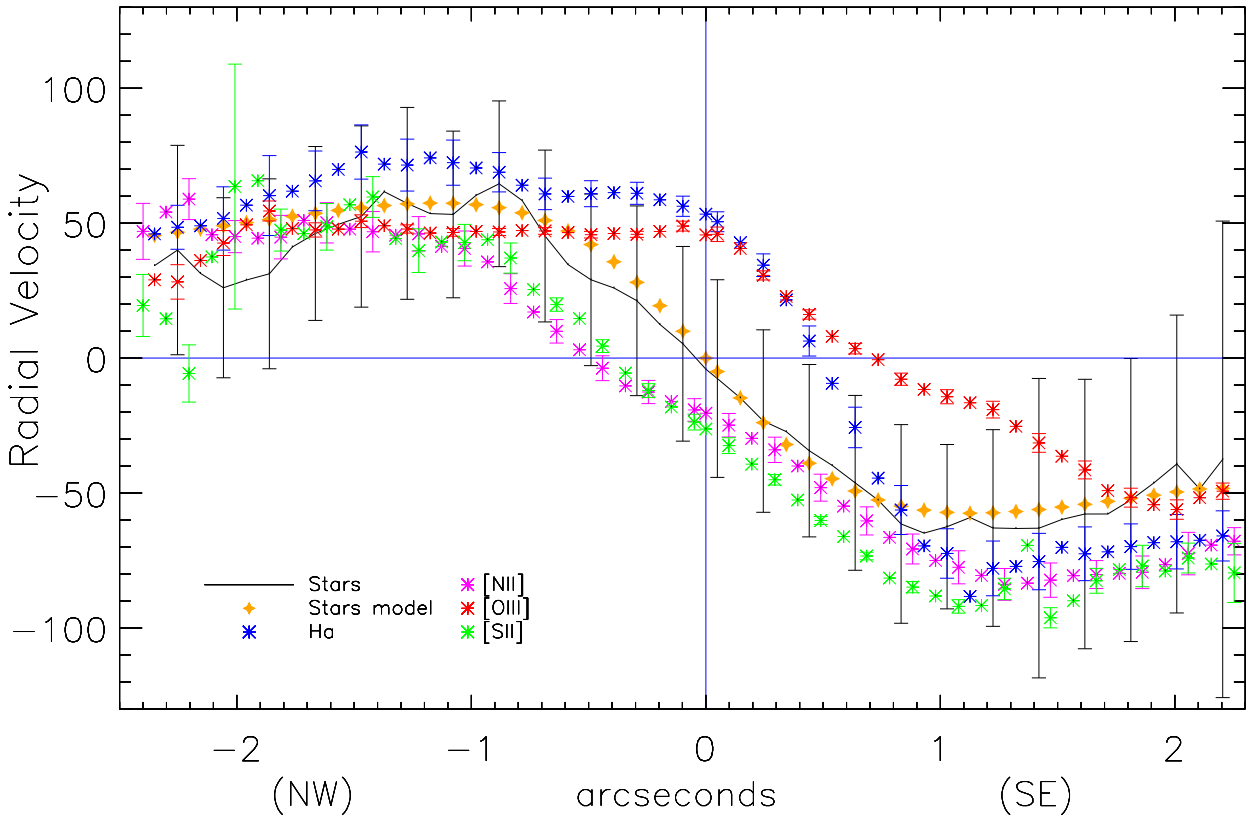

Radial velocities of the stronger emission lines along with the stellar velocity and its model.

Position velocity diagrams

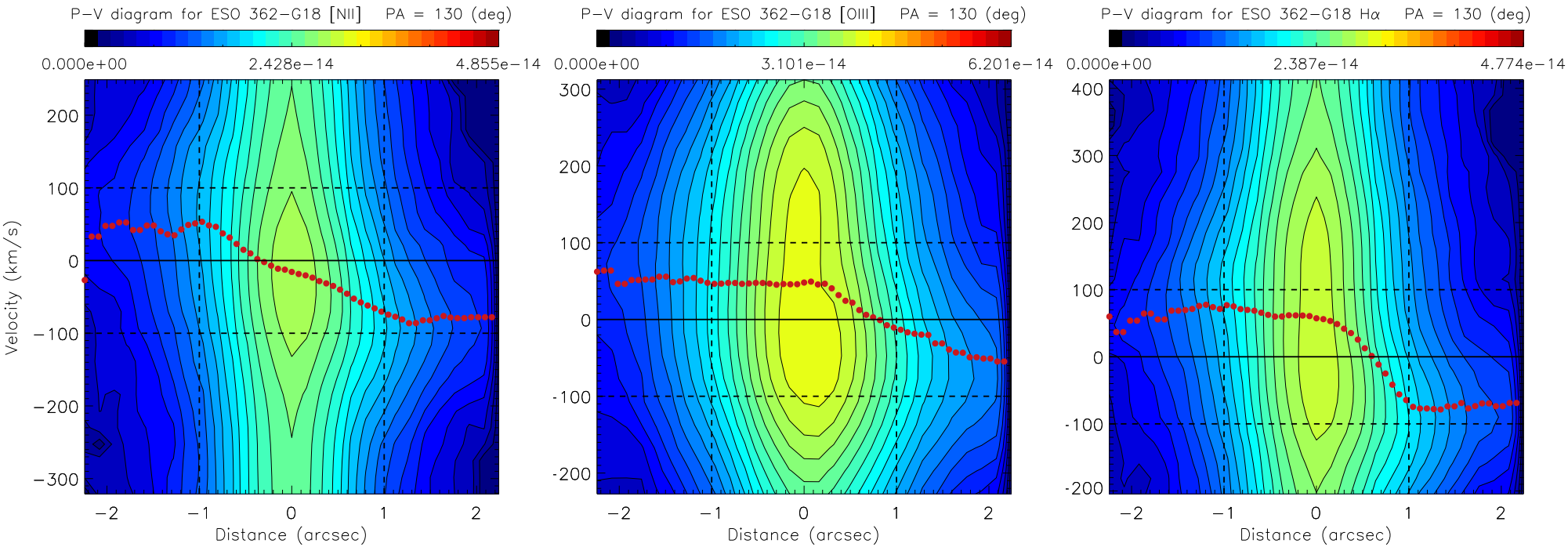

Position velocity diagrams for Hα, [O III] and [N II] emission lines.

Contours are in powers of $\sqrt{2}$.

Double Gaussian Fitting results

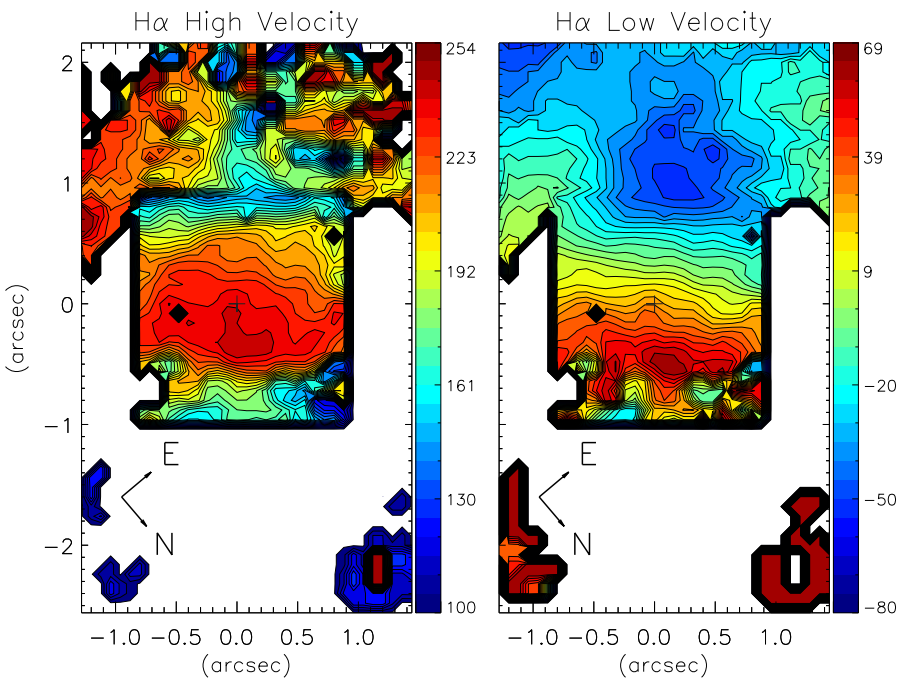

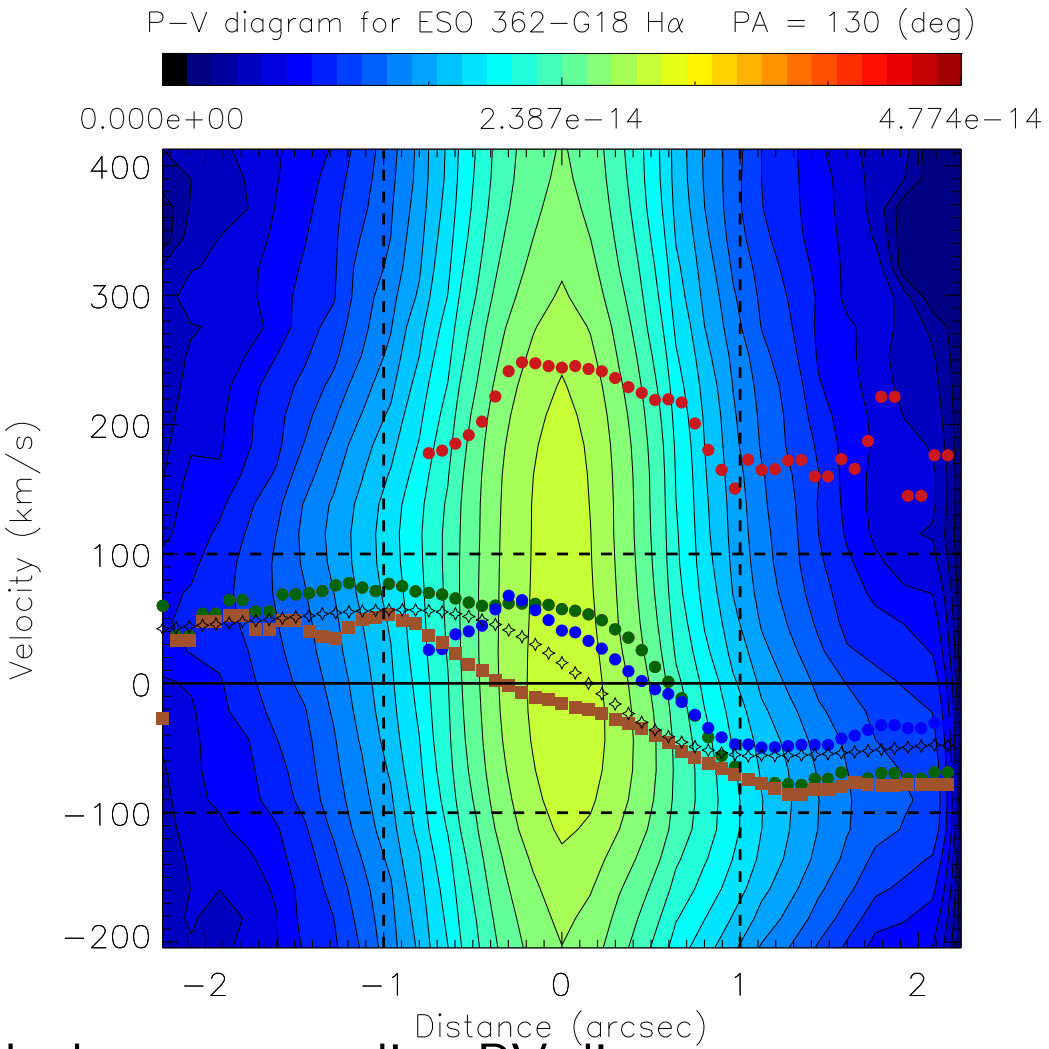

High and low Hα velocities along with the corresponding PV diagram.

Double Gaussian Fitting results

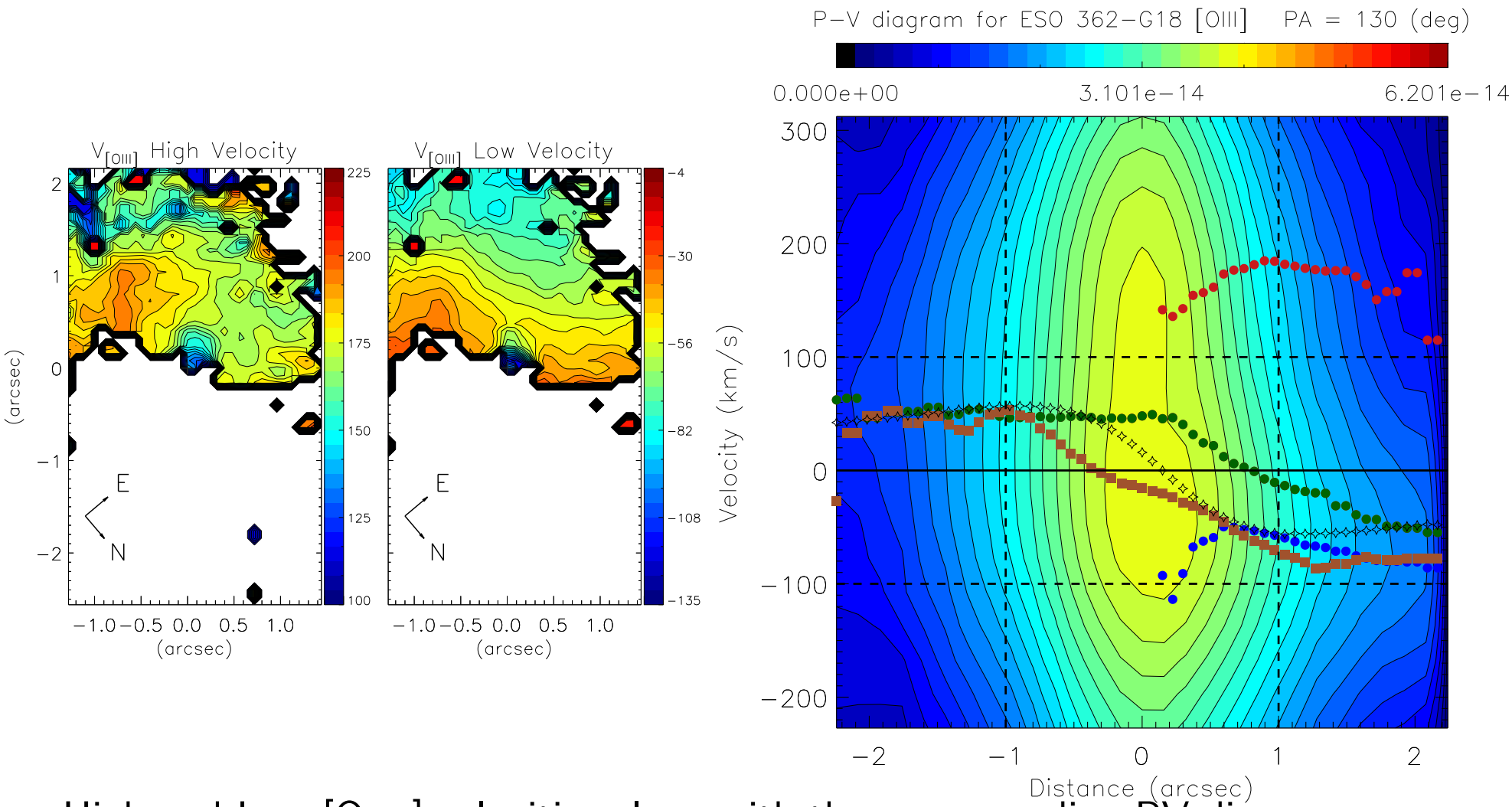

High and Low [O III] velocities along with the corresponding PV diagram.

Double Gaussian Fitting results

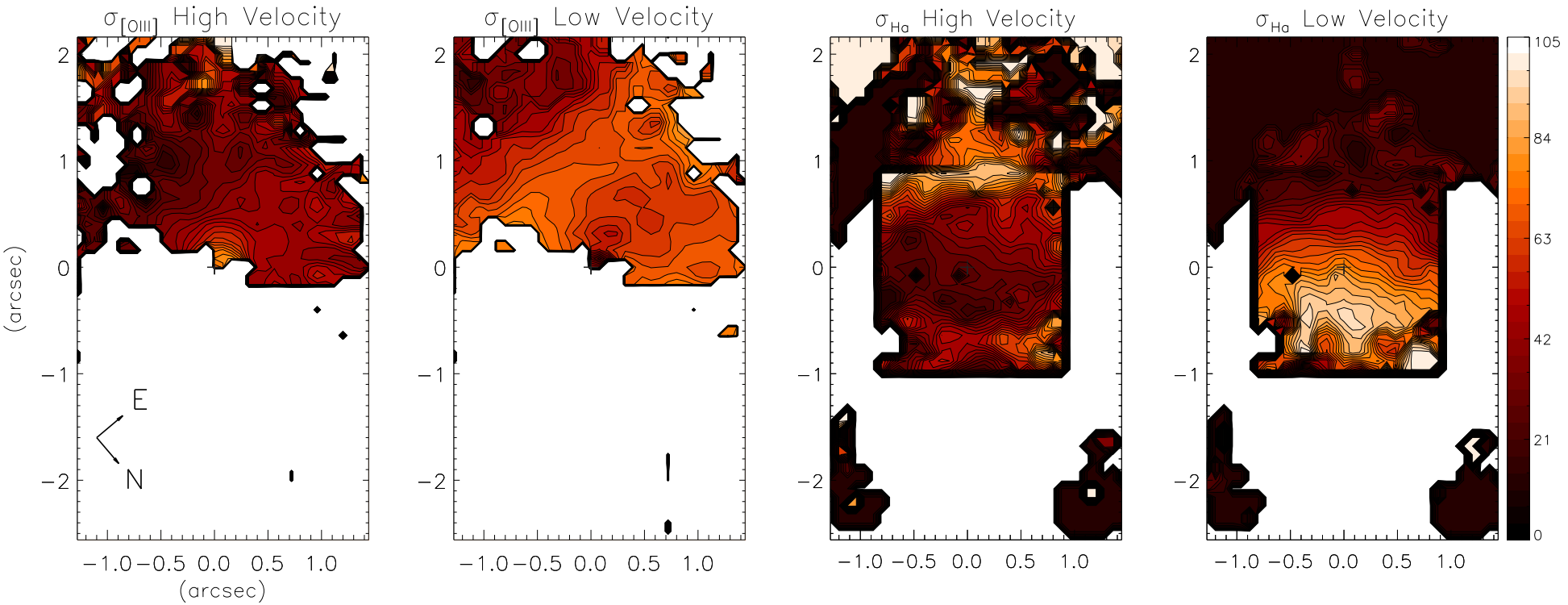

Velocity dispersions for each component in [O III] and Hα emission lines.

Double Gaussian Fitting results

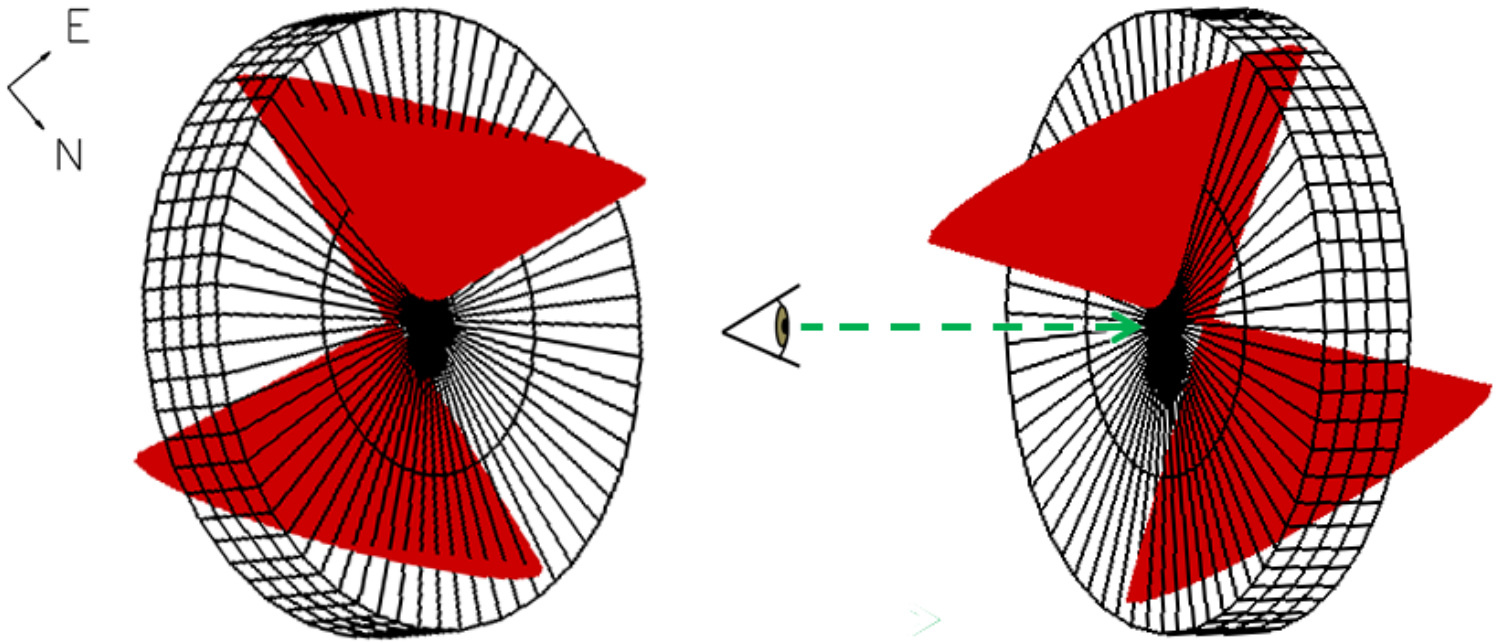

Biconical outflow model for ESO 362-G18. The galactic disk is shown from our field of view (left) and in profile (right).

Mass outflow rate

We can estimate the mass outflow rate ($\dot{M}$) as

$$\dot{M} = \frac{M_g}{t_d} \text{ , with } M_g = \frac{M_p L_{H\alpha}}{N_e j_{H\alpha}(T)} \text{ and } t_d = \frac{R_{out}}{V_{dep}},$$

where M_p is the proton mass, $L_{H\alpha}$ is the Hα luminosity of the outflowing material, N_e is the electron density and $j_{H\alpha}(T) = 3.3534 \times 10^{-25}$ erg cm^{-3} s^{-1} (Osterbrock, 1989); R_{out} is the radius of the outflow and V_{dep} is the mean deprojected velocity.

$$M_g = 1.5 \times 10^4 \text{ M}_\odot, \; t_d \sim 2 \times 10^5 \text{ yr}.$$

$$\rightarrow \dot{M} = 0.074 \text{ M}_\odot \text{ yr}^{-1} \rightsquigarrow 0.148 \text{ M}_\odot \text{ yr}^{-1} \checkmark$$

DEPARTAMENTO de ASTRONOMÍA UNIVERSIDAD DE CONCEPCIÓN

Mass accretion rate

$$\dot{M}_{acc} = \frac{L_{bol}}{\eta c^2} \ ,$$

Where $L_{bol} = 1.3 \times 10^{44}$ erg s^{-1} (Agís-González et al., 2014), c is the speed of light, and $\eta \approx 0.1$ (Shakura and Sunyaev, 1973).

$$\dot{M}_{acc} = 2.2 \times 10^{-2} \ M_{\odot} \ yr^{-1} \ ,$$

$$\frac{\dot{M}_{acc}}{\dot{M}} \sim 14\% \text{ (7 times smaller!!)}$$

$\therefore$ Most of the observed outflowing gas is mass entrained by the surrounding interstellar medium (Veilleux et al., 2005; Storchi-Bergmann, 2014).

DEPARTAMENTO de ASTRONOMÍA UNIVERSIDAD DE CONCEPCIÓN

Kinetic power

Simulations shown that the necessary energy budget for feedback, in order to affect a host galaxy, is 0.5% L_{bol} (Hopkins and Elvis, 2010). In ESO 362-G18, that amount is of:

$$\dot{E}_{out} = \frac{1}{2}\dot{M}(v^2 + 3\sigma^2)^* = 9.2 \times 10^{39} ergs^{-1}\ (0.007\%\ L_{bol}).$$

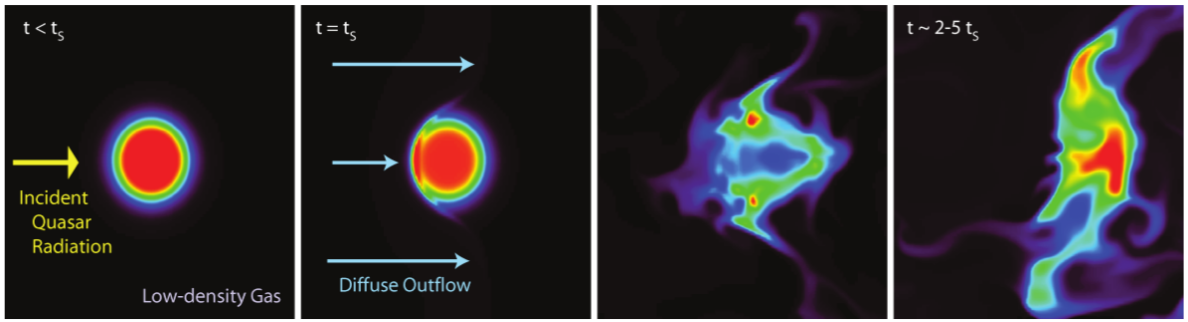

Effects of a two-stage feedback in a dense cloud of the ISM: at time $t = t_s$ is accelerated into a mach ~ 2 wind. At $t = 2 - 5t_s$ its effective cross-section is increased 10 times and, therefore, probably will be accelerated to $v \sim v_{esc}$ Hopkins and Elvis (2010).

*From Lena (2015)

kinetic power in agreement with previous results ✓

Different outflow/accretion parameters in the literature.

Galaxy	$\dot{M}_{out}$ ($M_\odot$ yr^{-1})	V_{out} (km s^{-1})	$\dot{M}_{acc}$ ($M_\odot$ yr^{-1})	$\dot{E}_{out}$ (10^{42} erg s^{-1})	L_{bol} (10^{42} erg s^{-1})	$\dot{E}_{out}/L_{bol}$	Ref
NGC 1068	9	1900 ± 80	0.015	5	88	0.05	1
NGC 2992	120	200 ± 20	0.015	2.5	85	0.029	1
NGC 3783	2.5	220 ± 20	0.003	0.07	180	0.0004	1
NGC 4151	2.4	600	0.013	0.24	73	0.0032	2
NGC 6814	7.5	120 ± 15	0.014	0.08	80	0.001	1
NGC 7469	4	130 ± 14	0.04	0.06	250	0.0002	1
NGC 1386	0.1	250	0.0003	0.0133	1.8	0.007	3
ESO 362-G18	0.15	394	0.013	0.0092	130	0.00007	⋆
NGC 2273	31.2	160-400	0.00009	0.0044	1.014	0.0043	4
NGC 3227	15.8	180	0.00073	0.00068	8.24	0.000082	4
NGC 3516	51	265	0.0041	0.0048	45.98	0.000104	4
NGC 4051	1.2	120-170	0.00011	0.000034	1.3	0.0000261	4
Mrk 1066	0.06	500	0.003	0.00601	17	0.0003535	5
Mrk 79	3.5	75	0.035	0.034	200	0.00017	6

References (Ref): (1) (Müller-Sánchez et al., 2011); (2) Storchi-Bergmann et al. (2010); (3) Lena et al. (2015); (4) Barbosa et al. (2009); (5) Riffel and Storchi-Bergmann (2011); (6) Riffel et al. (2013) and (⋆) this work.

DEPARTAMENTO de ASTRONOMÍA UNIVERSIDAD DE CONCEPCIÓN

Comparison with other works: Kinetic power, kinematic disturbances and dusty structures

- "Gaseous kinematics are more disturbed at small radii in the Seyfert galaxies compared with the inactive galaxies" Dumas et al. (2007) ✗

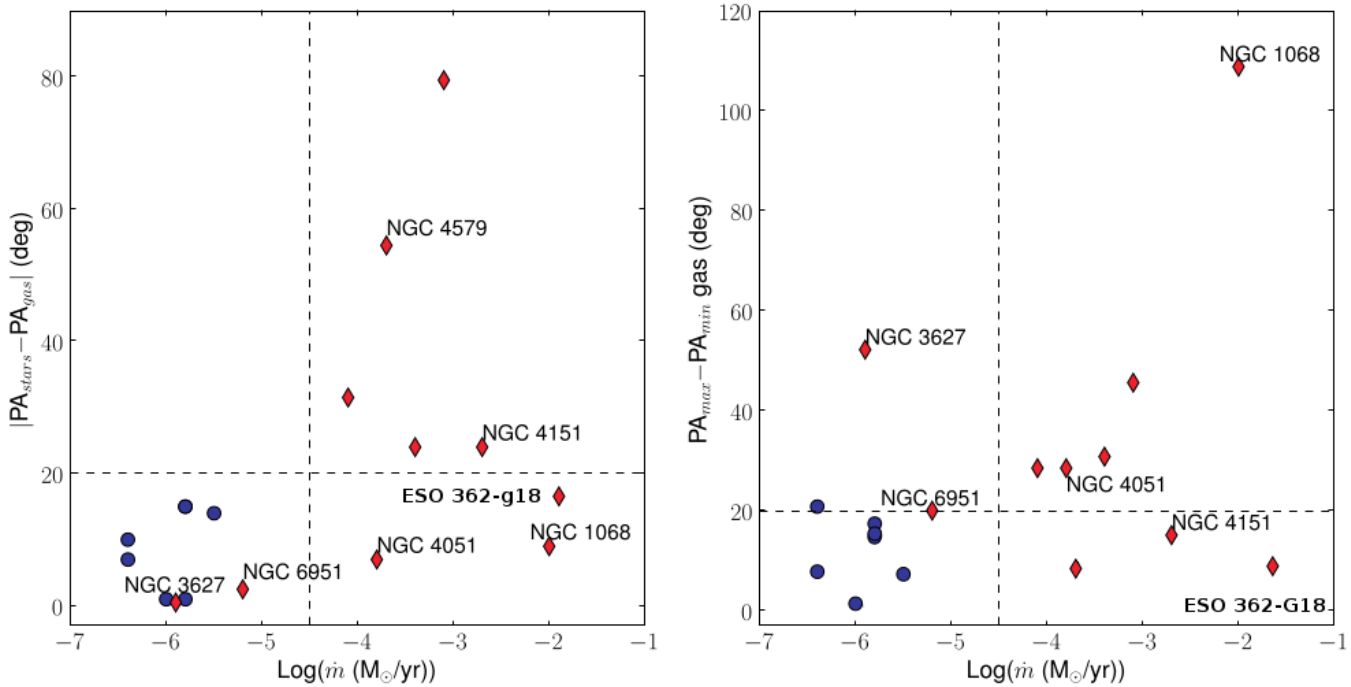

Kinematic disturbances measured by PA's variations between the gaseous and stellar kinematics (left) and maximum differences in the gaseous kinematics at different radius from the SMBH (right). Normal galaxies are in blue filled circles and active galaxies are red filled diamonds. The results for ESO 362-G18 were added for comparison. Modified from Dumas et al. (2007).

Comparison with other works: Kinetic power, kinematic disturbances and dusty structures

- "A clear connection between dust and AGNs in early-type galaxies" (Simões Lopes et al., 2007). ✓✗
- The presence of dust is a necessary, but not sufficient, feature for the activation of the nucleus in early-type galaxies (Davies et al., 2014). ✓

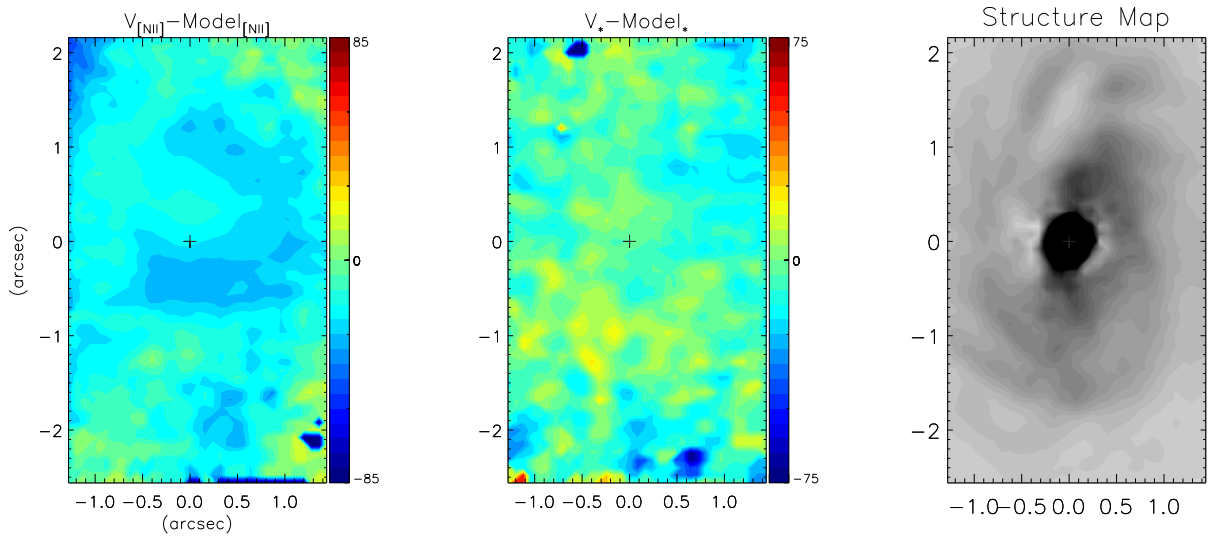

∴ The presence of dust does not imply an increased nuclear fuelling, confirming the second assertion also for this *Seyfert* galaxy.

Summary and conclusions

- A double Gaussian profile was fitted in [O III] and Hα emission lines in order to separate them in two kinematic components: a low-velocity component and a high-velocity component.
- The stars, the [N II] and [S II] emission lines, and the low-velocity component of Hα and [O III] lines, typically have radial velocities between -80 km s^{-1} and 70 km s^{-1} and have very similar rotation patterns, so we interpret all of these to originate in the rotating galactic disk.
- The high-velocity component of [O III] and Hα reach values in excess of 200 km s^{-1} with respect to the systemic velocity, and we argue that these spectral components originate from gas outflowing within the AGN radiation cone.
- The unusual dust morphology is probably a result of instabilities produced near the inner Lindblad resonance, which is expected within the inner 1.6 kpc. The presence of the dust structures also supports the hypothesis of Simões Lopes et al. (2007).
- While morphologically there is evidence that ESO 362-G18 is participating in a minor merger, we do not find any effect of this in the stellar or gas kinematics, within our relatively small FOV.
- Using the Hα luminosity, we estimate a lower limit for the mass outflow rate $\dot{M}$ of 0.074 M yr^{-1}. This value will double if a biconical outflow is assumed.
- The kinematic disturbances does not follow the trend expected by Dumas et al. (2007), who found that differences greater than 20° are common in AGNs and could be their activation mechanism.

DEPARTAMENTO de ASTRONOMÍA UNIVERSIDAD DE CONCEPCIÓN

References I

Agís-González, B., Miniutti, G., Kara, E., Fabian, A. C., Sanfrutos, M., Risaliti, G., Bianchi, S., Strotjohann, N. L., Saxton, R. D., and Parker, M. L. (2014). Black hole spin and size of the X-ray-emitting region(s) in the Seyfert 1.5 galaxy ESO 362-G18. *mnras*, 443:2862–2873.

Barbosa, F. K. B., Storchi-Bergmann, T., Cid Fernandes, R., Winge, C., and Schmitt, H. (2009). Gemini/GMOS IFU gas velocity 'tomography' of the narrow line region of nearby active galaxies. *mnras*, 396:2–18.

Bertola, F., Bettoni, D., Danziger, J., Sadler, E., Sparke, L., and de Zeeuw, T. (1991). Testing the gravitational field in elliptical galaxies - NGC 5077. *apj*, 373:369–390.

Davies, R. I., Maciejewski, W., Hicks, E. K. S., Emsellem, E., Erwin, P., Burtscher, L., Dumas, G., Lin, M., Malkan, M. A., Müller-Sánchez, F., Orban de Xivry, G., Rosario, D. J., Schnorr-Müller, A., and Tran, A. (2014). Fueling Active Galactic Nuclei. II. Spatially Resolved Molecular Inflows and Outflows. *apj*, 792:101.

Dumas, G., Mundell, C. G., Emsellem, E., and Nagar, N. M. (2007). Central kiloparsec of Seyfert and inactive host galaxies: a comparison of two-dimensional stellar and gaseous kinematics. *mnras*, 379:1249–1278.

Fathi, K. (2004). *Dynamics and morphology in the inner regions of spiral galaxies*. PhD thesis, University of Groningen.

Hopkins, P. F. and Elvis, M. (2010). Quasar feedback: more bang for your buck. *mnras*, 401:7–14.

Lena, D. (2015). *Aspects of Supermassive Black Hole Growth in Nearby Active Galactic Nuclei*. PhD thesis, Rochester Institute of Technology.

Lena, D., Robinson, A., Storchi-Bergman, T., Schnorr-Müller, A., Seelig, T., Riffel, R. A., Nagar, N. M., Couto, G. S., and Shadler, L. (2015). The Complex Gas Kinematics in the Nucleus of the Seyfert 2 Galaxy NGC 1386: Rotation, Outflows, and Inflows. *apj*, 806:84.

DEPARTAMENTO de ASTRONOMÍA UNIVERSIDAD DE CONCEPCIÓN

References II

Müller-Sánchez, F., Prieto, M. A., Hicks, E. K. S., Vives-Arias, H., Davies, R. I., Malkan, M., Tacconi, L. J., and Genzel, R. (2011). Outflows from Active Galactic Nuclei: Kinematics of the Narrow-line and Coronal-line Regions in Seyfert Galaxies. *apj*, 739:69.

Osterbrock, D. E. (1989). *Astrophysics of gaseous nebulae and active galactic nuclei*.

Riffel, R. A. and Storchi-Bergmann, T. (2011). Compact molecular disc and ionized gas outflows within 350 pc of the active nucleus of Mrk 1066. *mnras*, 411:469–486.

Riffel, R. A., Storchi-Bergmann, T., and Winge, C. (2013). Feeding versus feedback in AGNs from near-infrared IFU observations: the case of Mrk 79. *mnras*, 430:2249–2261.

Sánchez-Blázquez, P., Peletier, R. F., Jiménez-Vicente, J., Cardiel, N., Cenarro, A. J., Falcón-Barroso, J., Gorgas, J., Selam, S., and Vazdekis, A. (2006). Medium-resolution Isaac Newton Telescope library of empirical spectra. *mnras*, 371:703–718.

Shakura, N. I. and Sunyaev, R. A. (1973). Black Holes in Binary Systems: Observational Appearances. In Bradt, H. and Giacconi, R., editors, *X- and Gamma-Ray Astronomy*, volume 55 of *IAU Symposium*, page 155.

Simões Lopes, R. D., Storchi-Bergmann, T., de Fátima Saraiva, M., and Martini, P. (2007). A Strong Correlation between Circumnuclear Dust and Black Hole Accretion in Early-Type Galaxies. *apj*, 655:718–734.

Storchi-Bergmann, T. (2014). Active Galactic Nuclei at the Smallest Scales: Infall and Obscuration. In Creech-Eakman, M. J., Guzik, J. A., and Stencel, R. E., editors, *Resolving The Future Of Astronomy With Long-Baseline Interferometry*, volume 487 of *Astronomical Society of the Pacific Conference Series*, page 199.

Storchi-Bergmann, T., Lopes, R. D. S., McGregor, P. J., Riffel, R. A., Beck, T., and Martini, P. (2010). Feeding versus feedback in NGC4151 probed with Gemini NIFS - II. Kinematics. *mnras*, 402:819–835.

Veilleux, S., Cecil, G., and Bland-Hawthorn, J. (2005). Galactic Winds. *araa*, 43:769–826.

DEPARTAMENTO de ASTRONOMÍA UNIVERSIDAD DE CONCEPCIÓN

X-ray observation

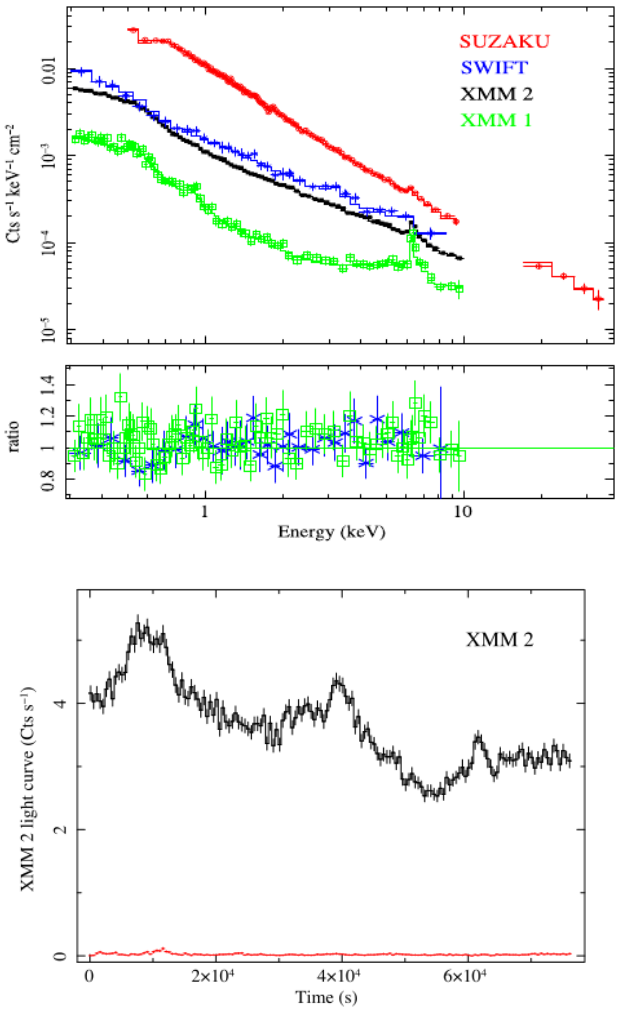

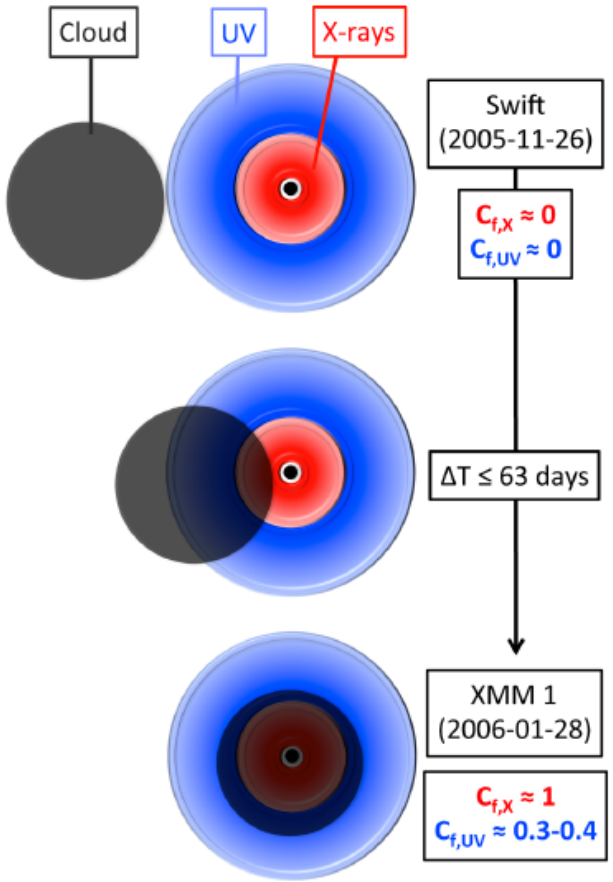

Agís-González et al. (2014)

Long-slit spectroscopy observation

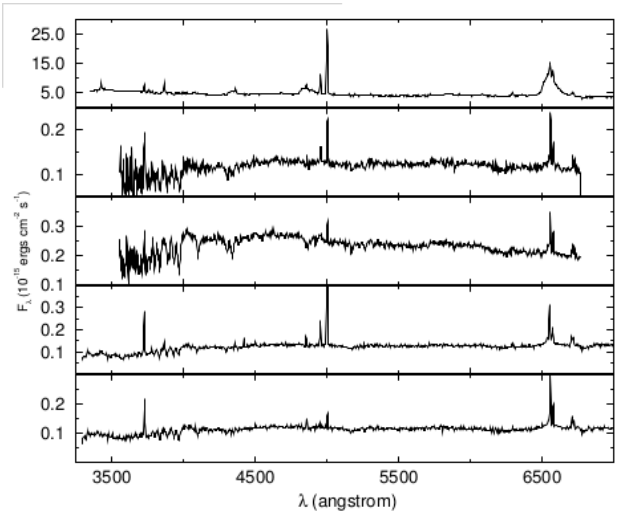

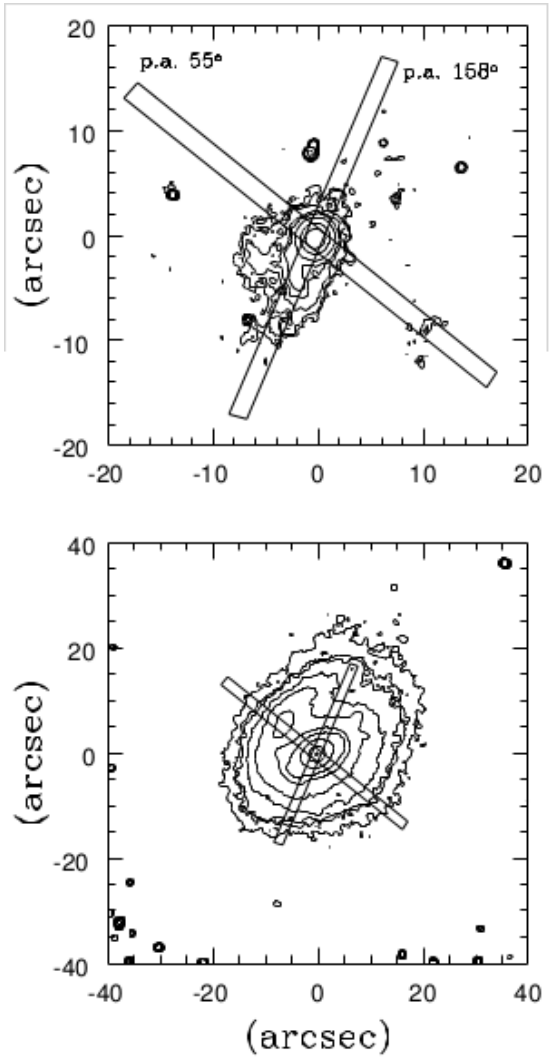

Fraquelli, Storchi-Bergmann, & Binette (2000)

Previous works about ESO 362-G18

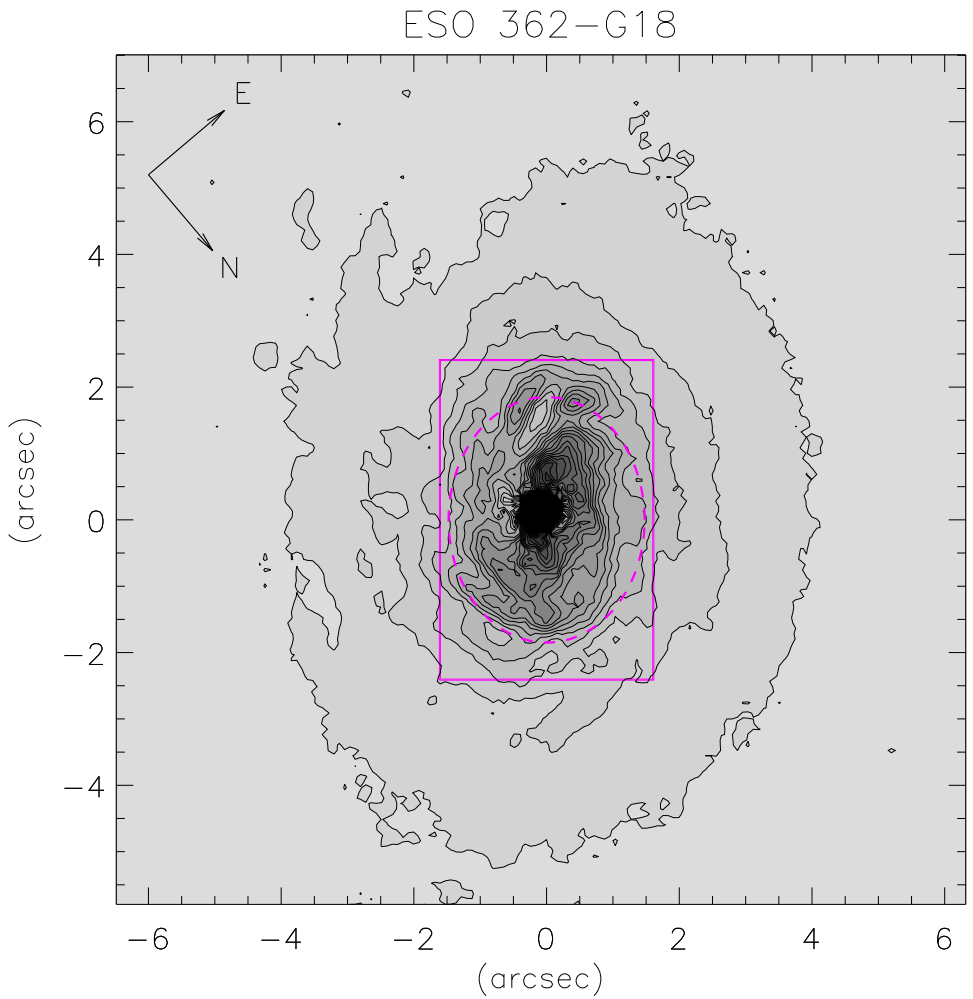

Structure map of ESO 362-G18 showing the posited minor merger. From this work.

pPXF

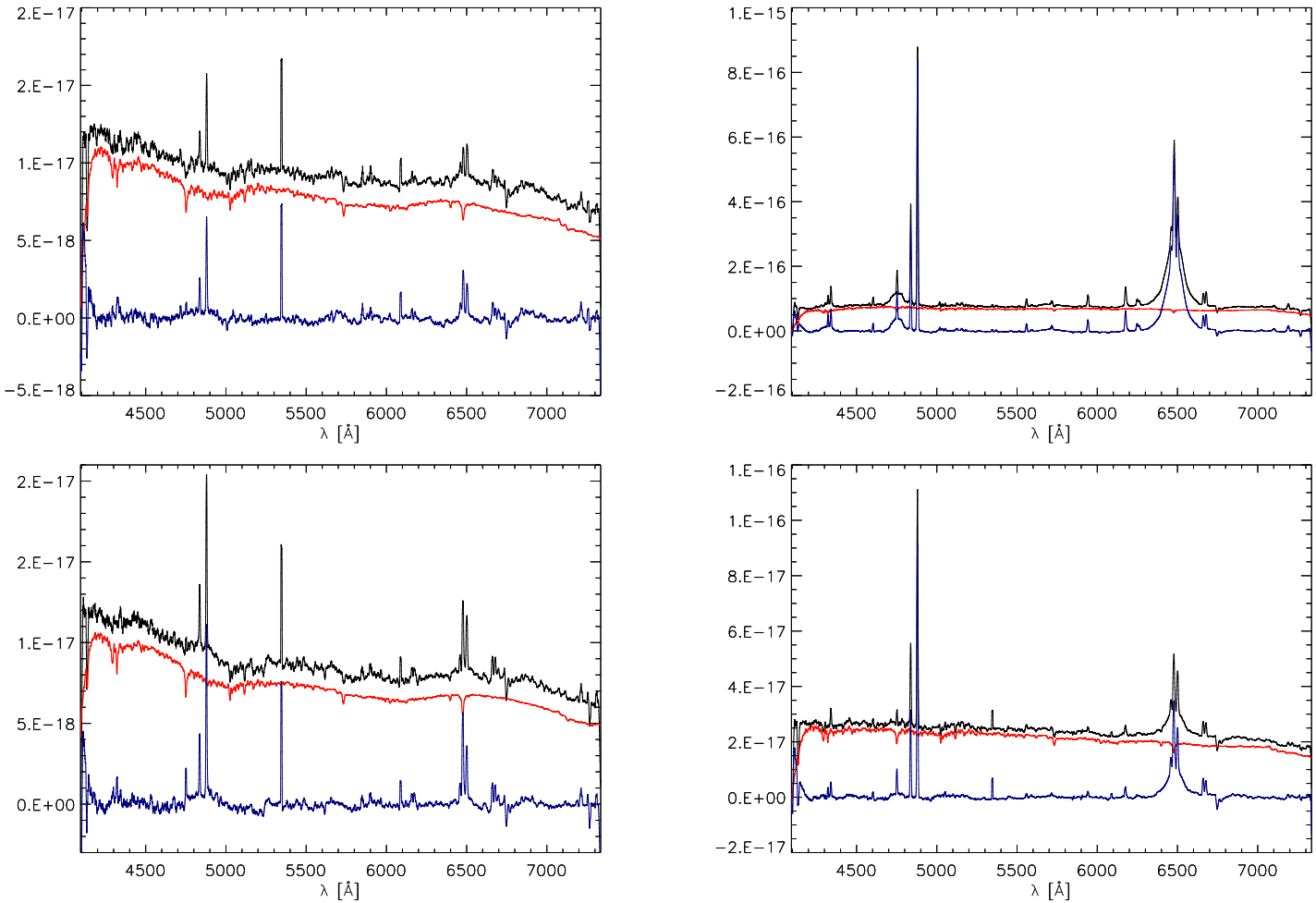

Continuum Fitting for ESO 362-G18 spectra using the MILES Stellar Library (Sánchez-Blázquez et al., 2006). Vertical axes are in erg cm^{-2} s^{-1} $Å^{-1}$.

DEPARTAMENTO de ASTRONOMÍA UNIVERSIDAD DE CONCEPCIÓN

Previous works about ESO 362-G18

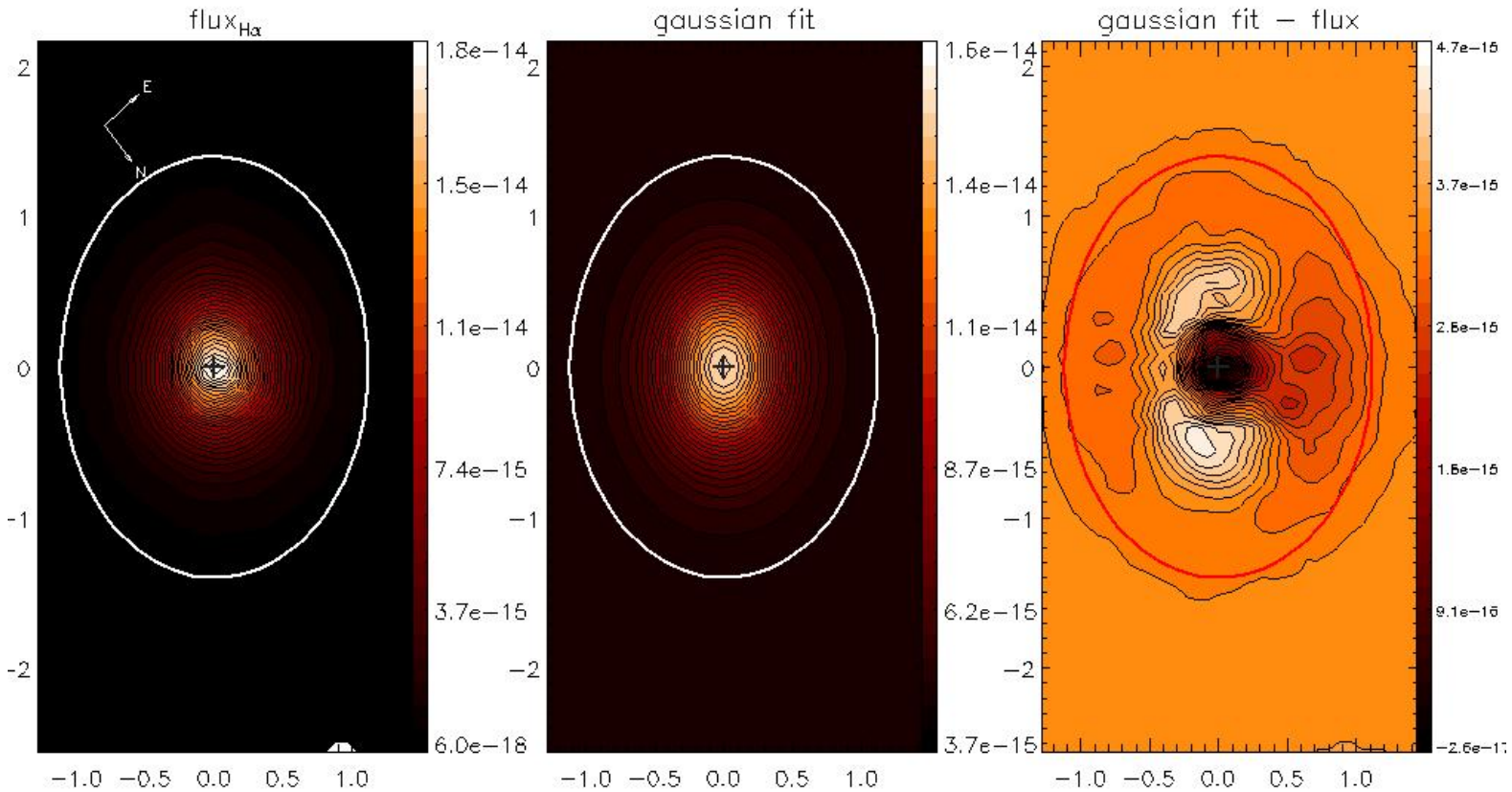

Flux inhomogenities in Hα. From this work.

Dusty structures

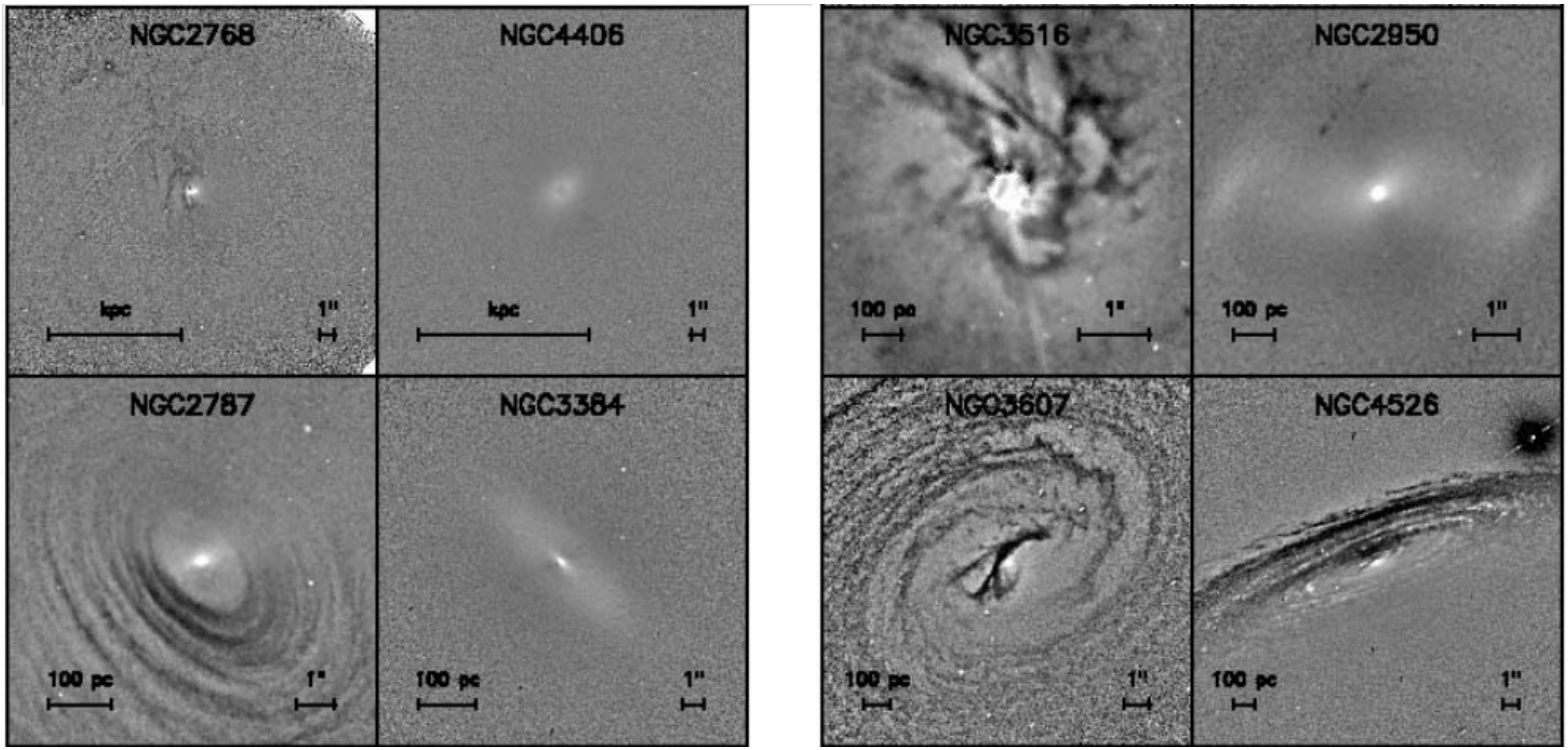

Dusty structures in active v/s non-active galaxies (Simões Lopes et al., 2007).

Previous works about ESO 362-G18

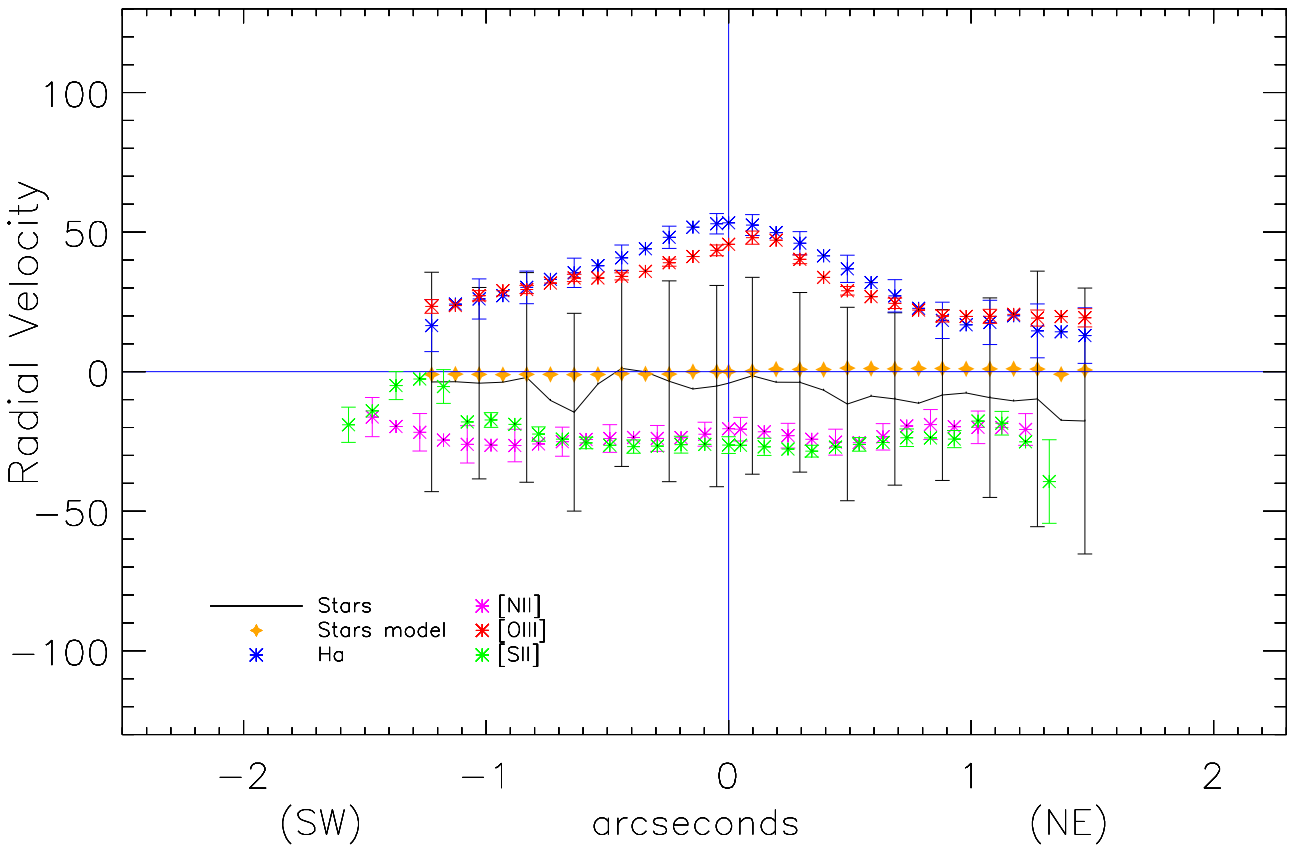

Radial velocities of the most prominent emission lines along their kinematic minor axis. From this work.

Previous works about ESO 362-G18

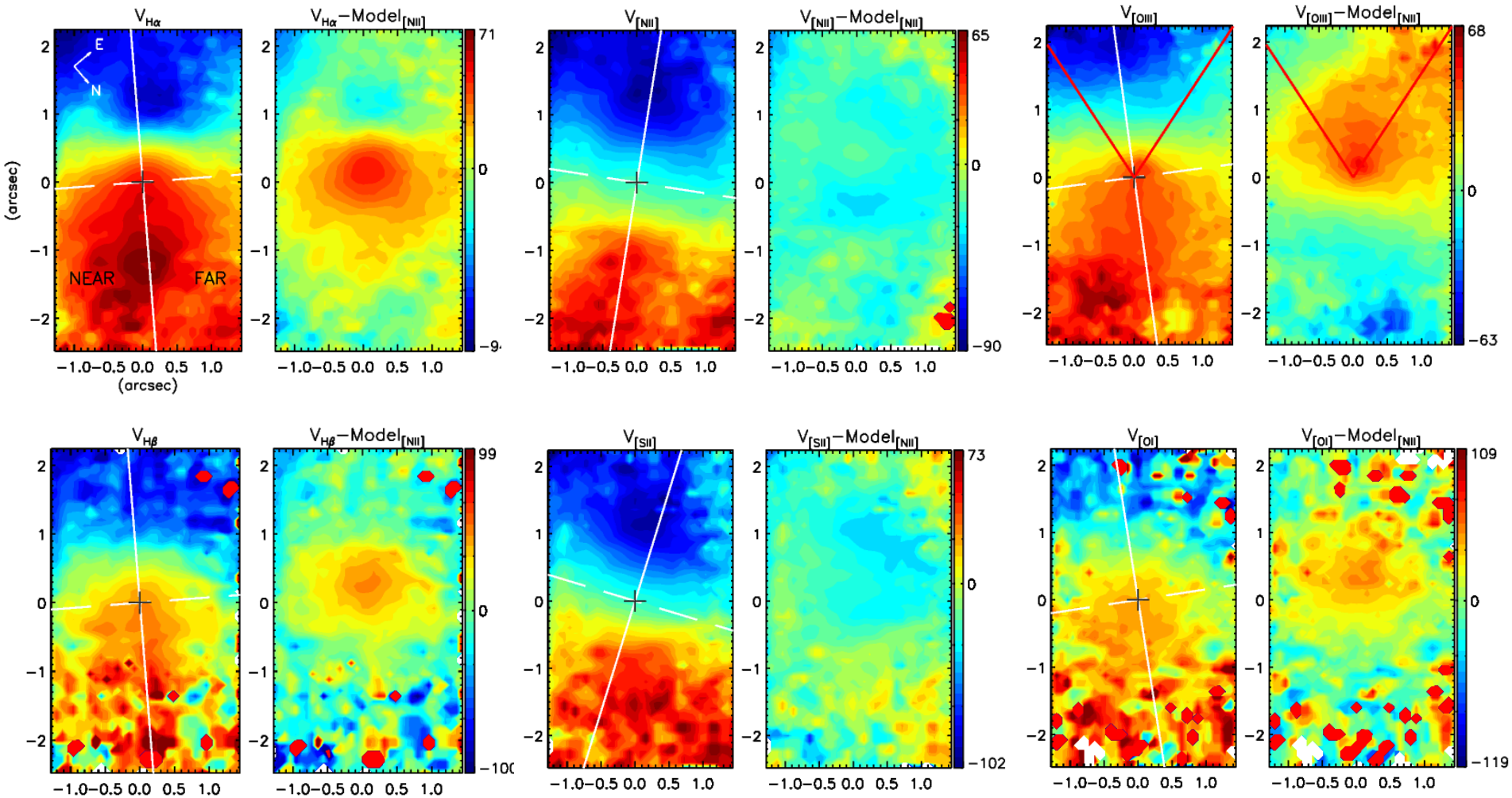

Comparison of similar gasous velocity fields (top with bottom panels). From this work.

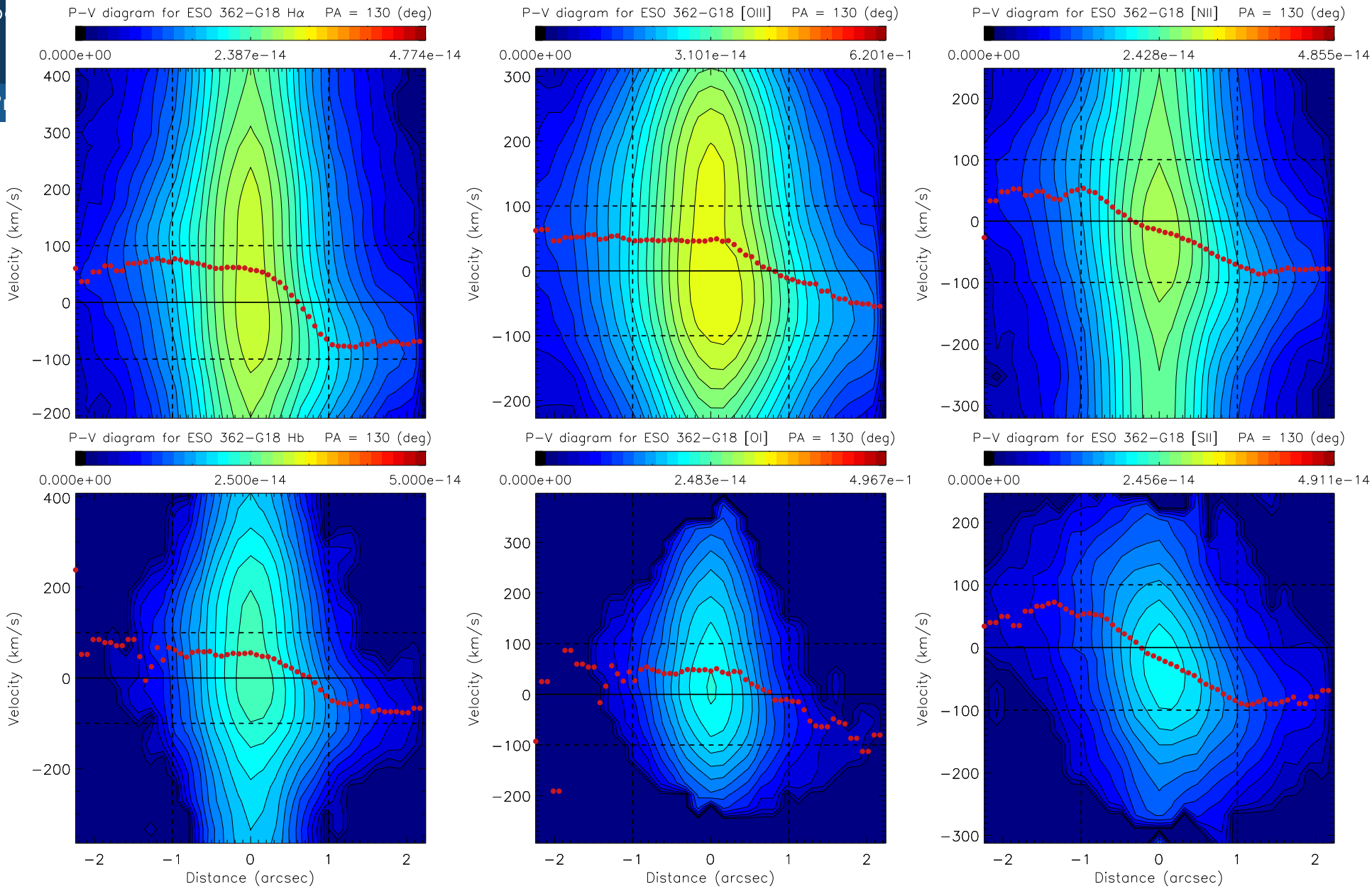

Comparison of similar position velocity diagrams (top with bottom panels). From this work.

Mergers and secular evolution

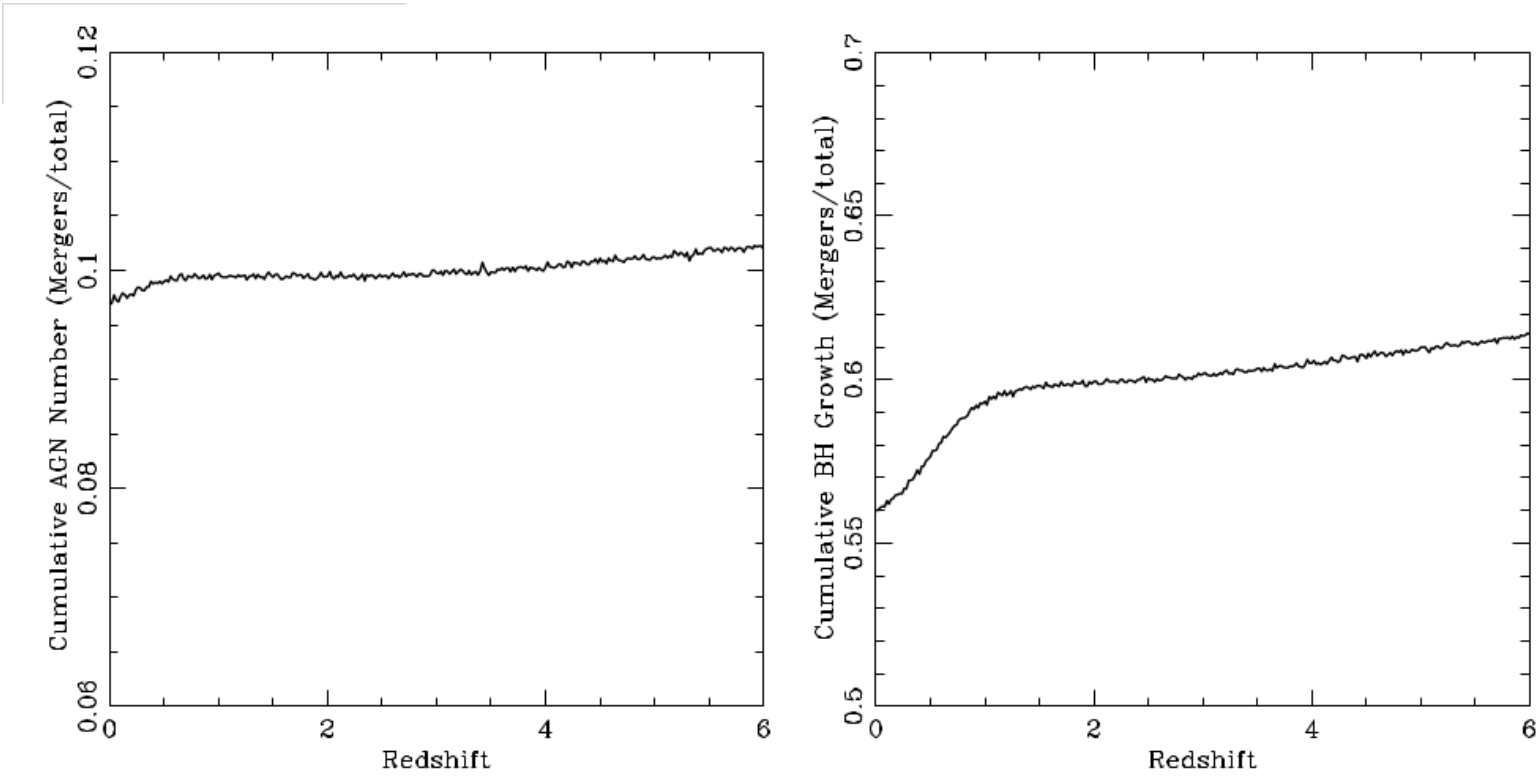

Mergers vs redshift (Treister et al. 2012).

Fluxer

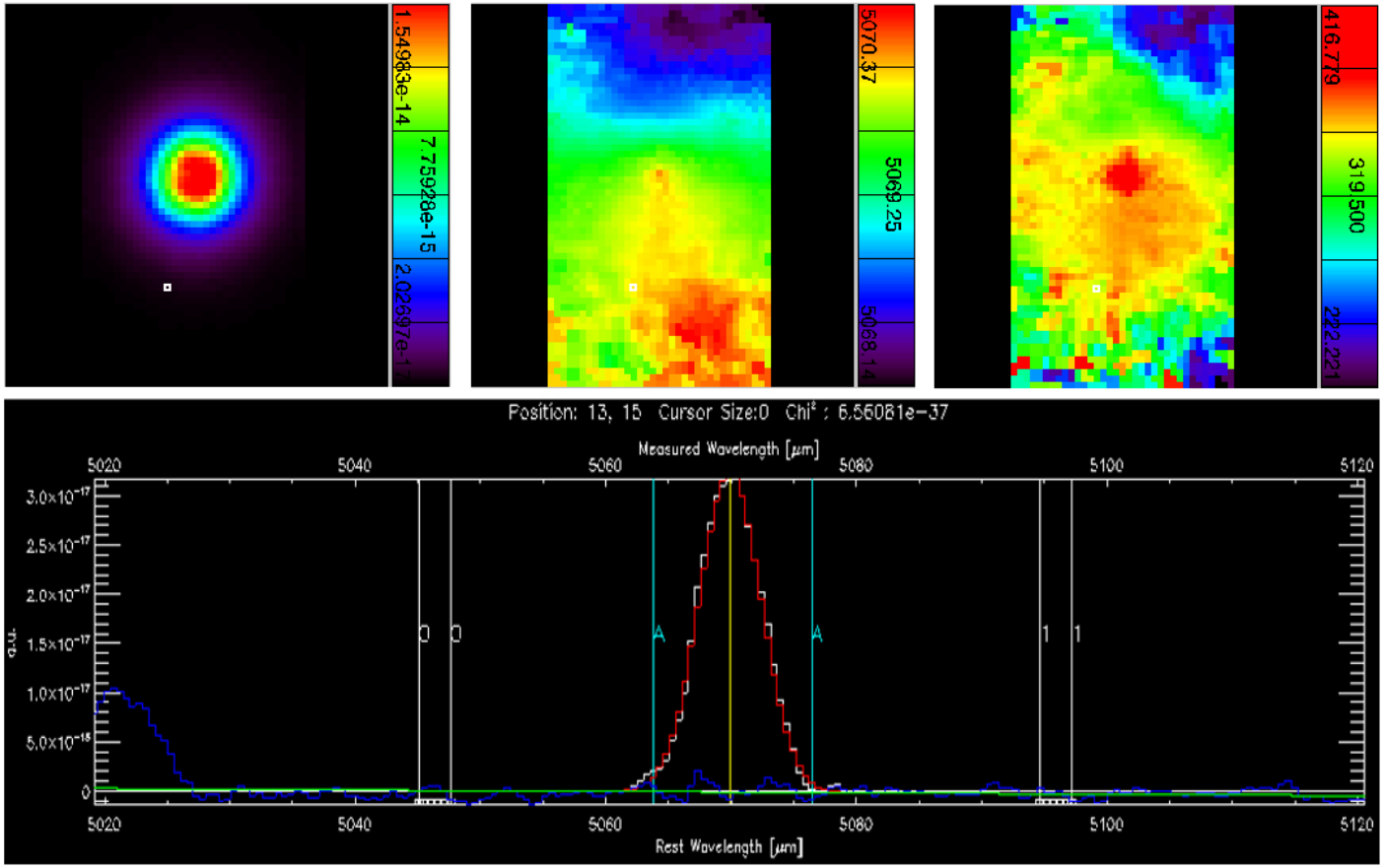

Single Gaussian fitting example performed with Fluxer by Cristof Iserlohe (http://www.ciserlohe.de/fluxer/fluxer.html).

Double Gaussian Fitting

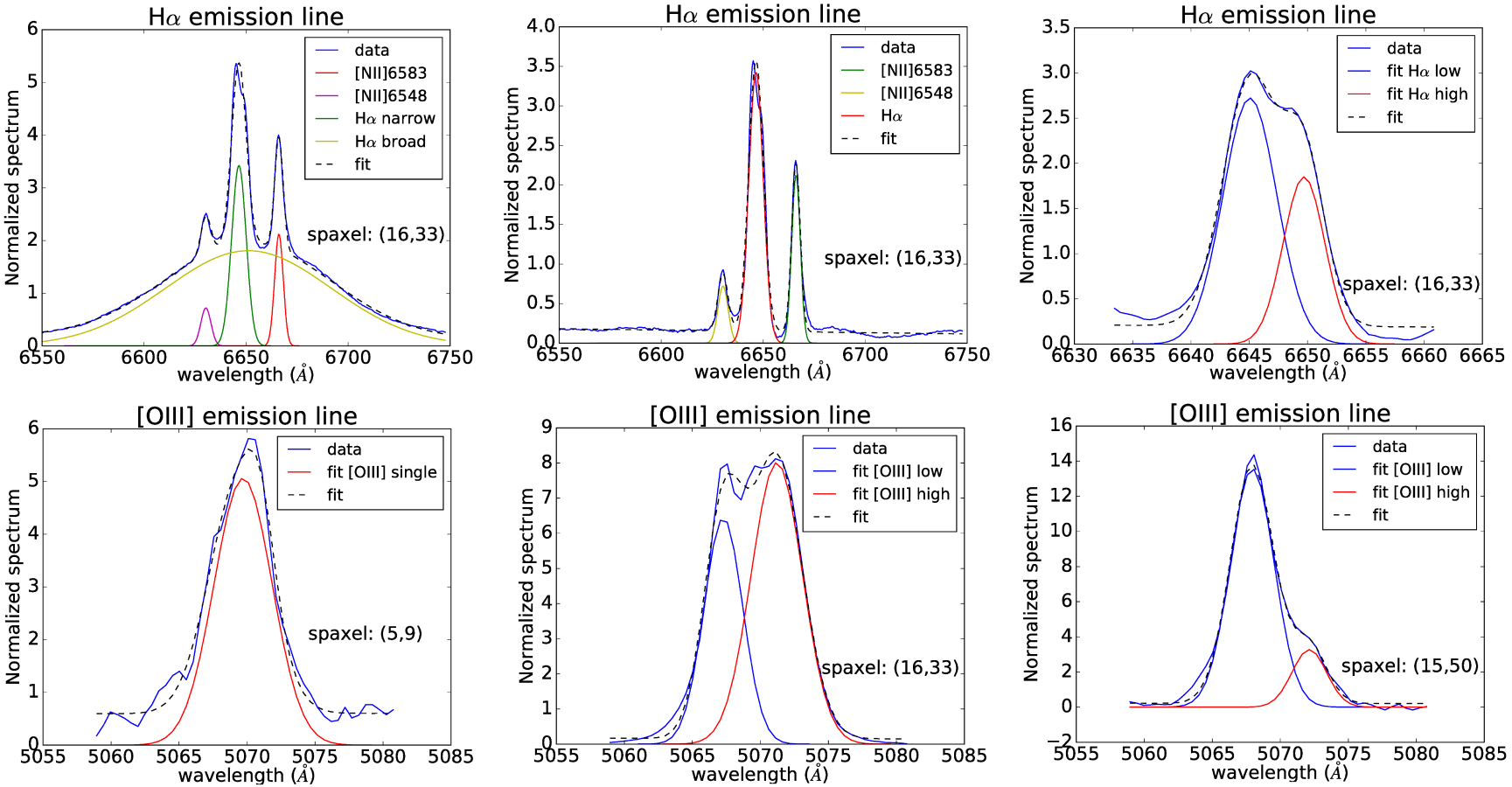

Example multiple Gaussian fits to the Hα+[N II] $\lambda\lambda$6548,6583 Å (upper panels) and [O III] λ5007 Å (bottom panels) normalized emission profiles.

DEPARTAMENTO de ASTRONOMÍA UNIVERSIDAD DE CONCEPCIÓN

Fluxes

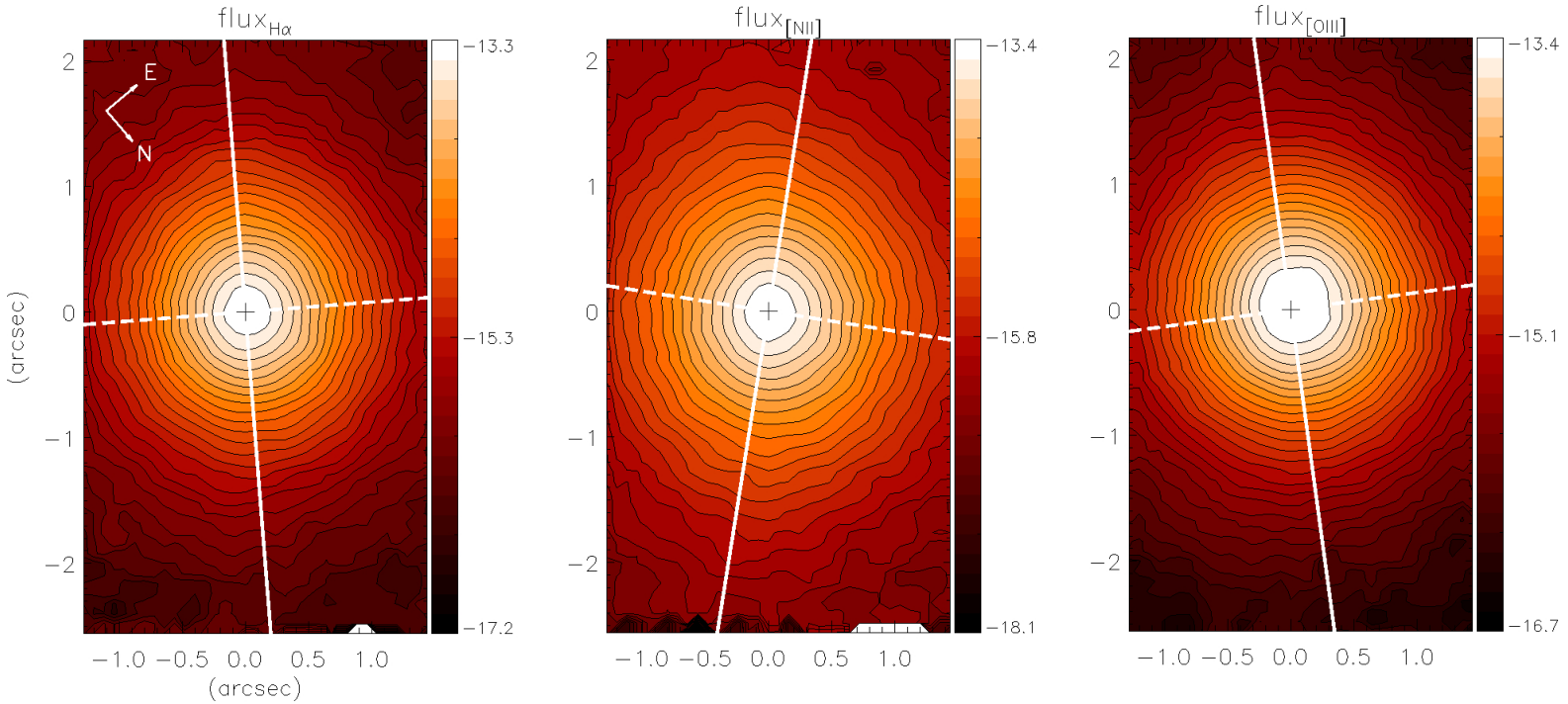

Maps of the Hα, [N III] and [O III] integrated fluxes (erg cm^{-2} s^{-1} per pixel) in logarithmic scale following the color bar to the right of each panel. No offset observed with respect to the continuum.

Electron density and emission line ratios

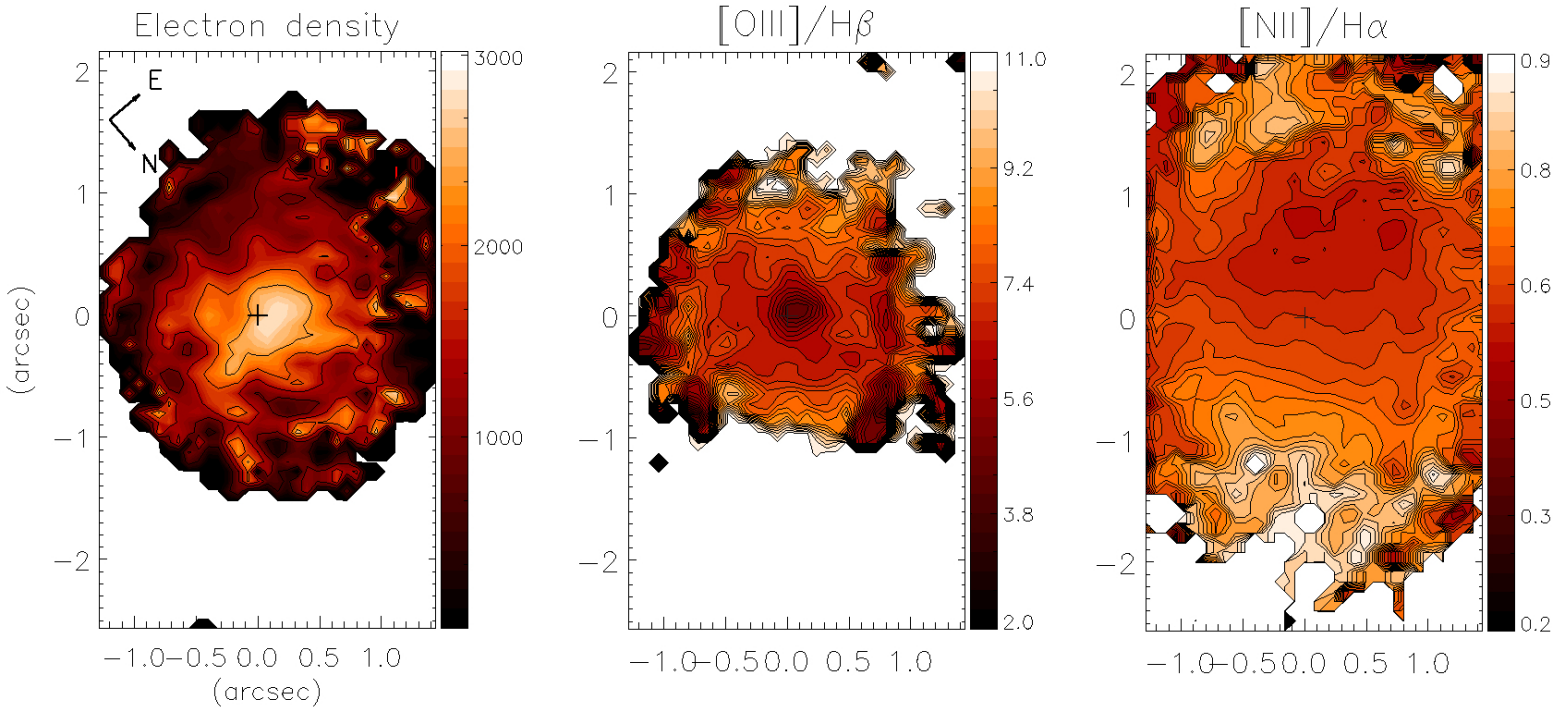

Maps of the estimated electron density (cm^{-3}) distribution and the line ratios [O III]/Hβ and [N II]/Hα, which are typical of AGNs, according to the BPT diagram.

Velocity dispersion

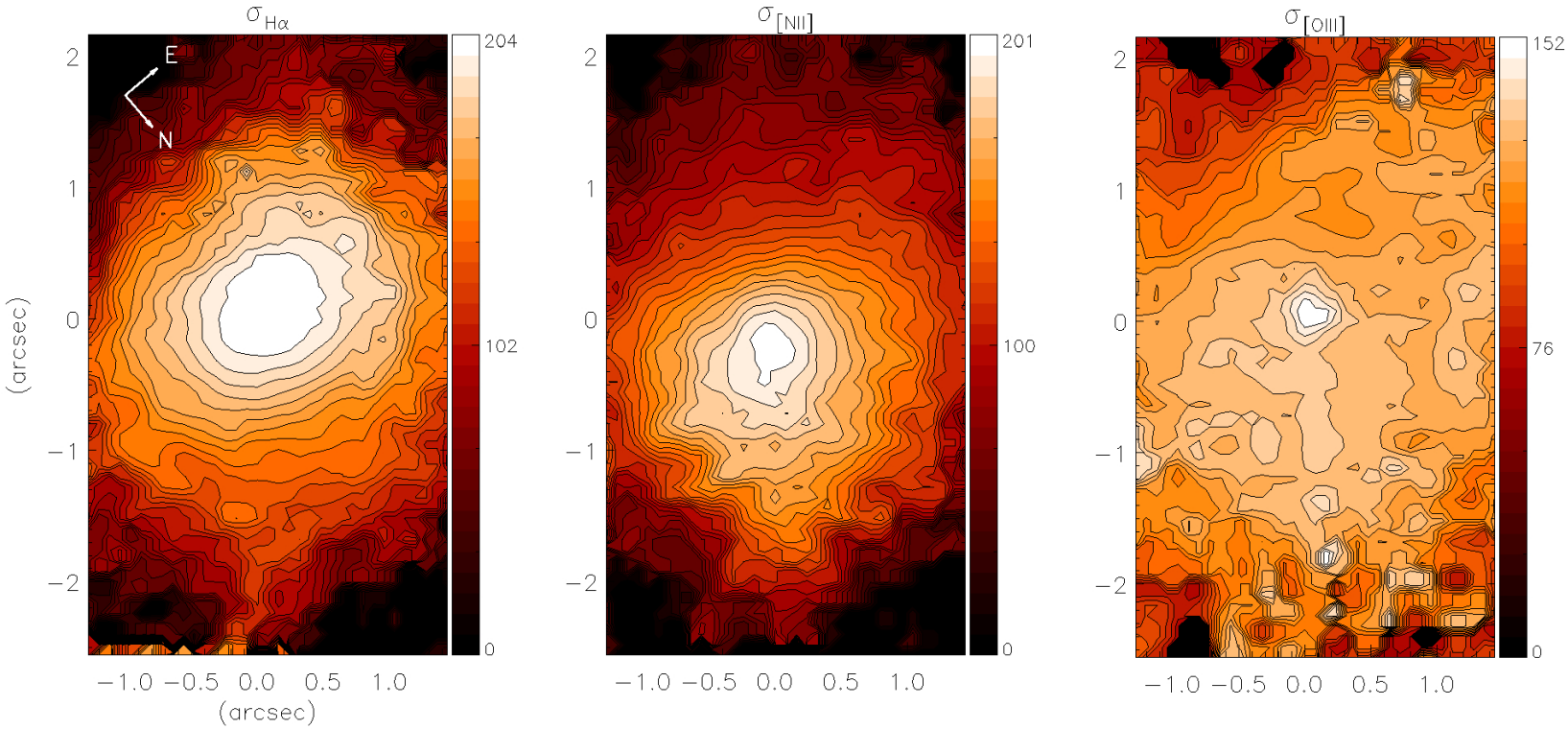

An important high dispersion component in Hα and [O III] is related to blended emission line profiles.